TAMPEREEN TEKNILLINEN YLIOPISTO
TAMPERE UNIVERSITY OF TECHNOLOGY

AYRTON PLAISIER

INFLUENCE OF SHADOWS CAUSED BY BUILDINGS ON THE POWER OUTPUT OF PHOTOVOLTAIC POWER GENERATORS

Master of Science Thesis

Examiner: prof. Seppo Valkealahti

Examiner and topic approved on 29 March 2017

ABSTRACT

Ayrton Plaisier: Influence of shadows caused by buildings on the power output of photovoltaic power generators.
Tampere University of technology
Master of Science Thesis, 67 pages
May 2017
Master's Degree Program in Electrical Engineering
Major: Electrical Engineering
Examiner: Professor Seppo Valkealahti
Keywords: Shadows caused by buildings, energy losses, photovoltaic

Shadows caused by clouds, trees, buildings and other structures cause the photovoltaic power installation to produce less energy. When installing a PV-generator these shadows should be taken into account when calculating the power output of this installation. Specifically the power losses from the shadows caused by trees and buildings should be avoided and can be predicted by calculations. If these energy losses are too big it is recommended to remove the object causing the shadow or to reposition the PV-installation.

In this thesis, the effect of shadows caused by buildings is examined more in detail because these shadows are very predictable and more easily simulated than shadows caused by trees or moving clouds. The goal is to achieve some values for the power and energy losses. For these simulations the same setup is always used so that the differences are more clear when different inputs for irradiance values are used.

As an input for the irradiance three different values have been used. As a first case a set value of 1000 W/m² has been chosen as the irradiance insolating the PV-installation. Because this value is constant the first simulations are more straightforward and don't take the fewer irradiance in the morning and evening into account. Secondly, the measured irradiance from the TUT PV-plant have been used. This data has been recorded for a couple of years now. The shadow caused by the building is then implemented in the irradiance curve from the selected day. Since there is data available from a couple of years already, the shadow can be added to clear sky days as well to cloudy days. The use of a cloudy day is used as the third case.

To see the influence of the shadow in a more practical way, the data from a whole month is used. Each day the building causes the shadow around noon when the losses are the highest. In this way the energy losses are more realistic than when only clear sky days are used to observe the losses.

PREFACE

The Master of Science Thesis has been done at the Department of Electrical Engineering of the Tampere University of Technology. The supervisor and examiner of the thesis was Professor Seppo Valkealahti.

First of all, I want to thank Professor Valkealahti for providing me this topic that goes very well together with my field of interest, renewable energy sources. I also want to thank him for the guidance and feedback during the production of this thesis. Furthermore, I want to thank pHd student Kari Lappalainen for the knowledge he passed on to me about Matlab programming and the use of his models in Simulink. Finally, I want to thank the international students and ESN INTO for the great atmosphere they provided during my stay in Finland.

Tampere, 17.4.2014

Ayrton Plaisier

LIST OF CONTENT

LIST OF SYMBOLS AND ABBREVIATIONS

Abbreviations

MML	Mismatch Losses
MPP	Maximum Power Point
MPPT	Maximum Power Point Tracking
OC voltage	Open-Circuit voltage
PV	Photovoltaic
SC current	Short-Circuit current
STC	Standard Testing Conditions

Symbols

A	Ideality factor
A_{bypass}	Ideality factor of a bypass diode
B	Temperature independent constant of saturation current
E_g	Band gap energy of semiconductors
E_{g0}	Linearly extrapolated zero temperature energy gap of a semiconductor
G	Irradiance
I'_{sc}	Short-circuit current without parasitic resistances
I_0	Saturation current of the diode in one-diode model of a photovoltaic cell
$I_{0,bypass}$	Saturation current of a bypass diode
I_{01}	Saturation current of the diode 1 in two-diode model of a photovoltaic cell
I_{02}	Saturation current of the diode 2 in two-diode model of a photovoltaic cell
I_{ph}	Light-generated current
I_{sc}	Short-circuit current
k	Boltzmann’s constant
K_I	Temperature coefficient of short-circuit current

K_T	Temperature-rise coefficient of open-circuit voltage
K_U	Temperature coefficient of a photovoltaic cell
N_s	Number of series-connected cells in a photovoltaic module
q	Elementary charge
r	Distance between PV installation and object causing shadow
R_s	Series resistance
$R_{s,bypass}$	Series resistance of a bypass diode
R_{sh}	Shunt resistance
T	Temperature
v	Speed of the shadow
V_{oc}; U_{oc}	Open-circuit voltage
x	Position of the shadow on the photovoltaic installation
γ	Temperature dependence of parameters of saturation current
ω	Angular velocity (of the sun)

1. INTRODUCTION

Since the start of the industrial revolution in the mid-1700s coal started to replace biomass as the main source of energy. Alongside a demographic explosion these two factors were the perfect cocktail for a world that is in need of an enormous amount of energy. Several oil crisis made it very clear that our dependence on oil became too big. Because of this, a worldwide interest for development of renewable energy sources grew. With the oil reserves depleting rapidly the EU has set different kind of targets. The 2020 targets are the most known. This package of targets concludes a 20% cut in greenhouse gas emissions (from1990 levels), a 20% improvement in energy efficiency and a minimum of 20% of the total EU energy should be produced by renewables. By 2030 these numbers should evolve respectively to 40%, 27% and 27%. One of the latest goals of the EU is the 2050 low-carbon economy. The content of this goal is again cutting the greenhouse gas emissions but now to 80% below 1990 levels. Also the emissions by 2040 should be cut with 60%. New to these 2050 targets is that all sectors have to contribute to achieve this goal. [2]

Today there are many kinds of renewable energy sources. Solar energy is one of them who has already been proven to be a promising one. Most people think about photovoltaic panels when they hear solar energy. The photovoltaic cells use the irradiance of the sun and converts this directly into electrical energy. But this is only one of the two methods that are available today. If lenses or mirrors are used to focus a large area of sunlight into a small beam then the method of using solar energy is called concentrated solar power. Photovoltaic cells however have become economically profitable for households and companies since 6 to 7 years. The ‘module price per Watt’ in 1976 was around 84 dollar while in 2015 it was 0.7 dollar. Because of this decline in price the installed amount of photovoltaic installations has grown enormously. In 2014 an amount of 177 GW of PV installations was installed globally while in 2015 that number was 227 GW. [3]

Photovoltaic power generators consist of series and parallel-connected PV panels or modules. The purpose of the series connection is to increase the voltage level of the

installation. If it concerns an installation that has to be connected to the grid a high voltage is required. The parallel connection of the PV modules is mandatory to achieve a higher current for the PV installation. When different levels of irradiance reach the surface of the photovoltaic installation, the operation of this generator can undergo harmful effects. These effects are more crucial with a series connection. When one module is shaded while the rest of the series connection remains unshaded then the total current will be limited to the current produced by the shaded module. Problems start to occur if the total current of the series connection is higher than the short-circuit current of the shaded module. A part of the power that is produced by the non-shaded modules will then be dissipated in the shaded one which may lead to damage to the module. This problem can be solved by adding anti-parallel bypass diodes that allows the current to bypass the shaded panels so the current is not limited. Every coin has two sides and so has this solution. These bypass diodes can lead to multiple power points in the voltage-power curve. Because of this the maximum power point tracking techniques need to be advanced enough. [6] [4]

The main goal of this thesis is to study the influence of shadows caused by buildings on the power or energy output of the PV installation and not to determine the effects of different parameters that influence the irradiance on the PV panels. For this reason the inclination of the panels, height of the sun and other parameters influencing the irradiance are neglected and only the measured irradiance data from the TUT Solar PV research plant is used. The parameters used in this thesis are those for the NAPS NP190GKg PV module. The model which was received from PhD student Kari Lappalainen is used in MATLAB Simulink and is based on the model presented by Villalva et al. In this thesis a certain setup is used for the building causing the shadow that will cover the PV installation. For the input irradiance different values have been chosen, one of these values is the measured data from the TUT PV installation.

This thesis consists of several chapters. The first one contains background information about solar energy and the basics of photovoltaic power production. This chapter is important to understand the following chapters of the thesis. Chapter 3 will explain which PV generator and studied system setup are used for the simulations performed in MATLAB Simulink. All the results are gathered in chapter 4 as well as the conclusions found by these results.

2. BACKGROUND INFORMATION

In this chapter all the necessary background information will be provided to understand everything explained further in this thesis. In short it contains some basic solar energy information and the basics of photovoltaic power production.

2.1 Solar energy and the photoelectric effect

Solar power is one of the most important source of energy nowadays. Each year the upper atmosphere of the earth receives 174000 terawatts of solar radiation [10]. Approximately 30% of that is reflected back to outer space while the rest of that radiation gets absorbed by clouds, land masses and seas. [1]

Atoms are composed of core with positive charged protons and neutrons, and a shell with negative electrons. If a photon with enough energy from incident light hits an electron then the photon can be absorbed by the electron. When the external photoelectric effect is considered, the electron is able to leave the material if the photon carries the amount of energy that is necessary for this electron to leave the material. In solar cells who are made of semiconductors there is also an internal photoelectric effect. Basically when a photon has a sufficient amount of energy then it can lift an electron from the valence band to the conduction band. The amount of energy needed for this process is called the band gap energy E_g. This band gap energy is shown in figure 1. [8] [6]

The electron-hole pairs generation in pure semiconductors is caused by the internal photoelectric effect. However due to the missing force that separates electrons and holes, the recombination is strong. To make the PV cells produce power a junction is needed which can separate the electrons and holes. The simplest kind of junction that can be used is the p-n junction. [6] The p-n junction contains a strong electric field. This is because the concentration difference when a p-type semiconductor and a n-type semiconductor are connected together. Negative electrons will diffuse from the n-type region to the p-type region which leaves behind a positively charged n-type region. The positive holes will diffuse from the p-type region to the n-type region and leave behind a negative p-

type region. This diffusion has as a result that an electric field has been produced. The electric field wants to counteract the diffusion. Because of this a drift current is induced opposite of the diffuse current. When there is thermal equilibrium than the drift current is the same as the diffuse current so that there is no net current flowing through the junction. In this junction there are no mobile charge carriers and this region is called the depletion region. [6] [4]

If in the valence band of a p-type semiconductor an electron receives enough energy from a photon then an electron-hole pair will be created. The negative electron was excited to the conduction band of the p-type semiconductor and, as a result of the electric field of the depletion region, pulled to an n-type semiconductor. When this p-n junction gets connected to an external load, electrons will return from the n-type to the p-type semiconductor through the load and so electrical power is produced. [6] [4]

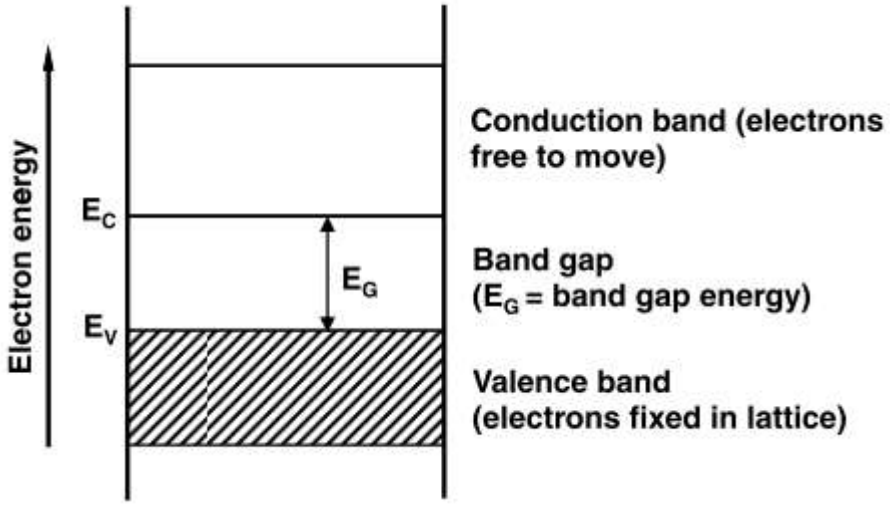

Figure 1. Semiconductor band model. The width of band gap energy E_g is determined by the semiconductor material used. [4]

2.2 Basics of solar power production

In this subchapter some basics about solar power production will be explained. The way PV modules are connected has an influence on the behavior of the PV installation. When the PV installation is partially shaded it will react according to how it is connected and how many bypass diodes are used. Finally in this chapter the modelling of a PV module will be explained.

2.2.1 Series connection of PV modules

When connecting PV panels in series, the main goal is to obtain a higher and usable voltage. To observe the behaviour of a series connection of photovoltaic panels some simulations have been performed. In figure 2 the voltage-current curve and voltage-power curve of 1 panel, 2 panels and 3 panels in series is shown. All three panels are exposed to an irradiation of 800 W/m² while the temperature of them is chosen to be 25 °C. Since the irradiance for all three panels is the same, their short-circuit current is also equal.

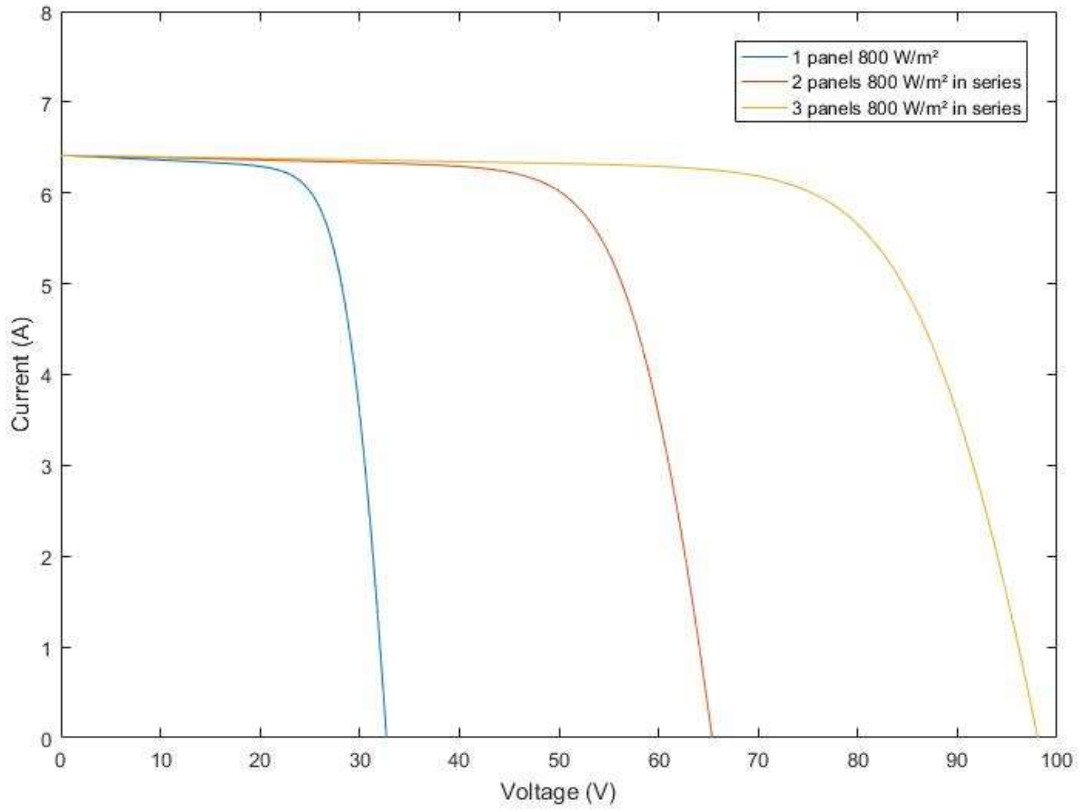

Figure 2. Voltage current curve of series connection of PV modules with an irradiation of 800 W/m².

The voltage of the series connection of 3 panels is received by adding the voltage of the two panels to the voltage of the single panel. Since the panels are connected in series the current for the three panels is the same but the voltage is the sum of every individual PV panel. The result for the power-voltage curve is evident. Since the voltage is a multiplication of the voltage produced by one PV panel, the power curve will also

rise, linear to the amount of panels connected in series. The voltage-power curve for 1 and 2 and 3 panels connected in series under 800 W/m² irradiance is shown in figure 3.

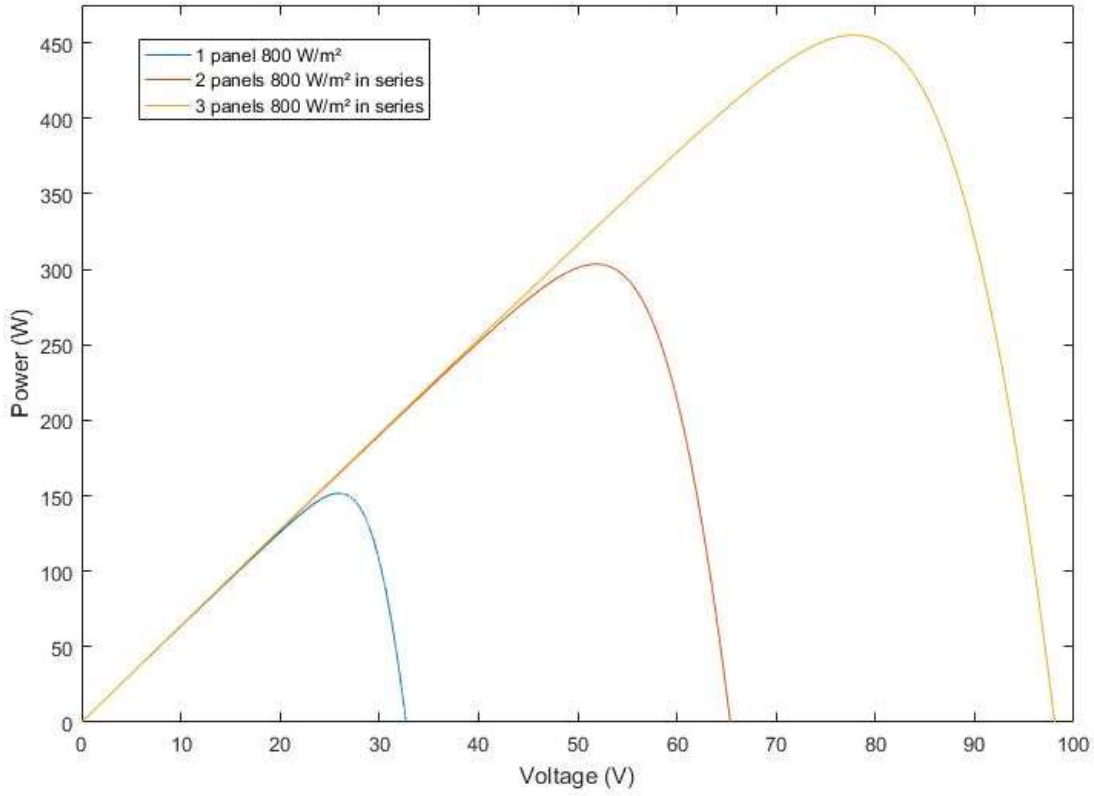

Figure 3. Voltage-power curve of 1 PV module, 2 PV modules connected in series and 3PV modules connected in series. The irradiation of every panel is 800 W/m².

If there is a series connection between two panels with different irradiation, the current voltage curve is as in figure 4. In this case both the solar panels have a bypass diode since the current from the series connection is not limited to the current of the PV panel with only 500 W/m² irradiation. This bypass diode is necessary to avoid hot-spots and thus damage to the PV panel who is shaded.

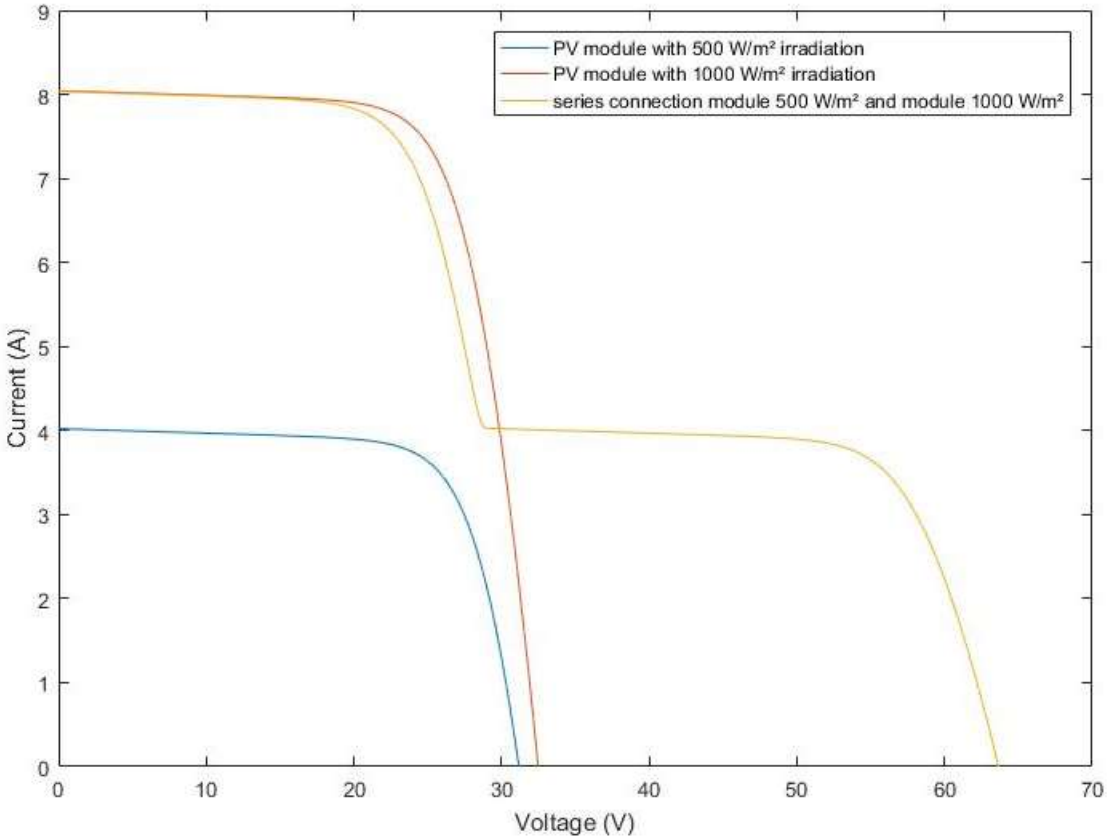

Figure 4. Voltage-current curve of a series connection of a PV module with 500 W/m² irradiation and a PV module with 1000 W/m². The modules both have a bypass diode.

If there is a series connection between a PV-panel with an irradiance of 1000 W/m² and a PV panel with an irradiance of 500 W/m² the power-voltage curve shown in figure 5 will occur. It is clearly visible that there are now 2 Maximum Power Points or MPP's. The local MPP is situated around 20 V and 6.3 A. The global MPP is located at 56 V and 3.2 A.

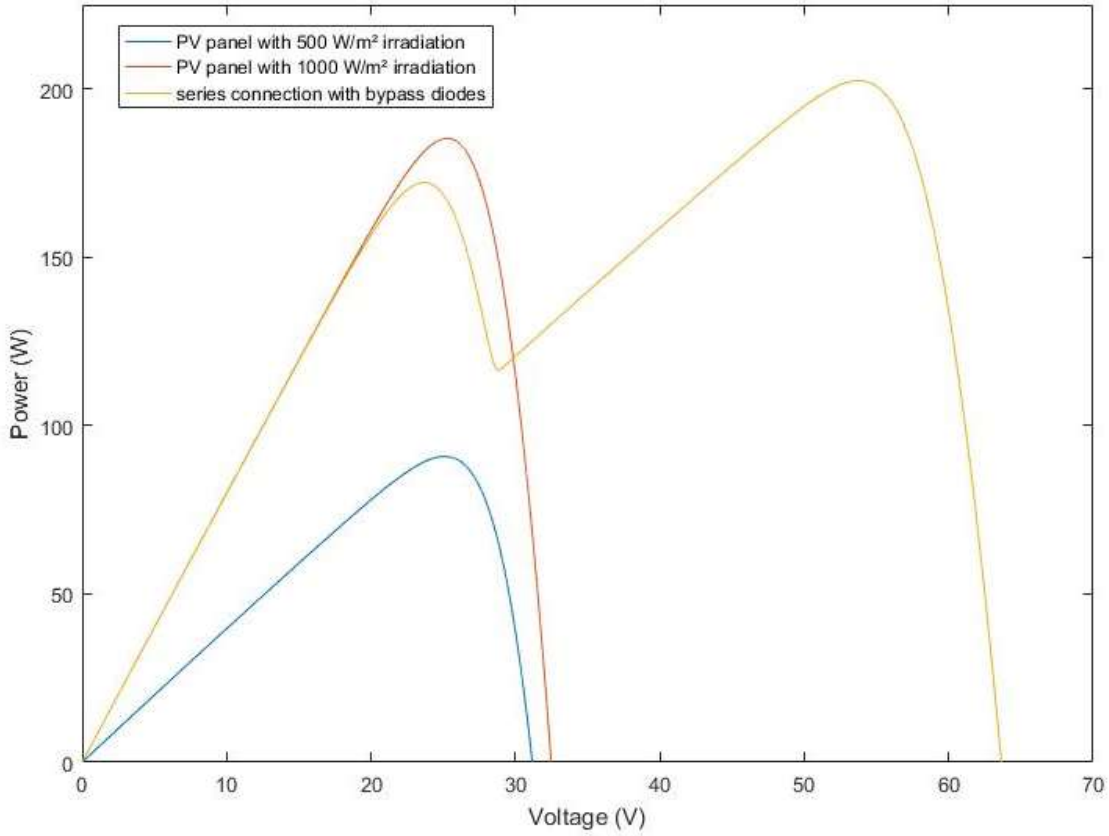

Figure 5. Voltage-Power curve for the series connection of a PV module with 500 W/m² irradiation and a PV module with 1000 W/m². The modules both have a bypass diode.

When simple MPPT (maximum power point tracking) techniques are used, it is possible that they keep tracking the local MPP instead of the global one. In this case the power output of the PV-generator can enormously be reduced. This will be more clear when the results of a shadow passing by a PV-generator will be evaluated later on in this thesis. [4]

2.2.2 Parallel connection of PV modules

When connecting PV modules in parallel the short-circuit current of each individual panel can be added up. The open-circuit voltage (OC voltage) remains the same unless the cell temperature of the cells differs. In that case the OC voltage of the hotter cell will be a little less than the colder one. The parallel connection will have an OC voltage value somewhere in between the value of the cold and hot cell. Later in this thesis the effect of temperature will be discussed and it is visible there that the OC voltage rises if the cell is colder. The voltage-current curve of a parallel connection can be seen in figure 6.

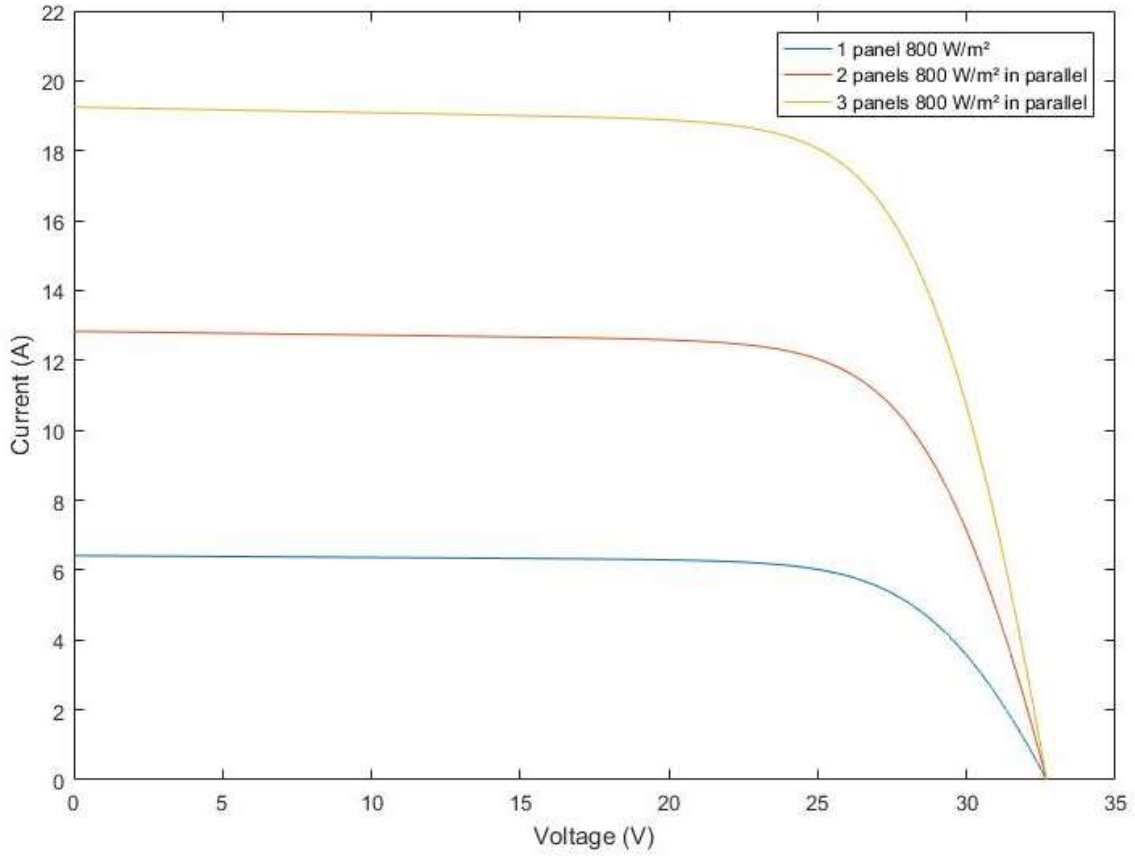

Figure 6. Voltage-current curve for a parallel connection of PV modules with an irradiation of 800 W/m² each.

The voltage-power curve for a parallel connection of PV modules can be seen in figure 7. The maximum power of the parallel connection rises linear with the amount of PV modules being added to the PV installation.

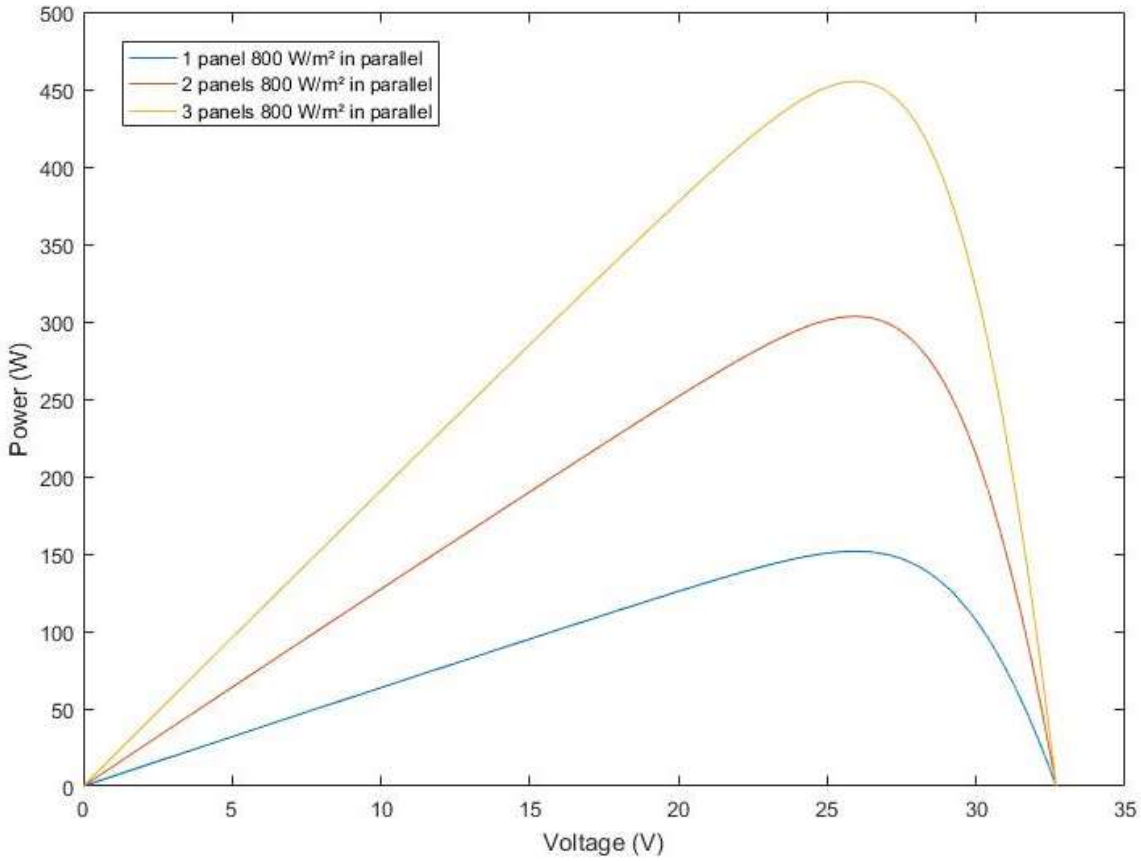

Figure 7. Voltage-Power curve for a parallel connection of PV modules with an irradiation of 800 W/m² each.

2.2.3 Wiring problems

When wiring solar modules it is important that the individual cells are protected from unusual operating conditions. These could cause overload or overheating which results in damage to the individual cell. A closer look to the operation curves of a solar cell gives us more clarification.

The active area of the solar cell is the fourth quadrant. This region is reached when sunlight insolates on the solar panel. When due to an external effect the current starts exceeding I_{sc}, the voltage in the cell will become negative. This causes the solar cell to

start operating in the third quadrant is the reverse direction of the diode. The situation is different when the voltage exceeds the V_{oc}. In this case the solar cell starts operating in the passband direction of the diode, also the first quadrant. The characteristics of the solar cell are presented in figure 8.

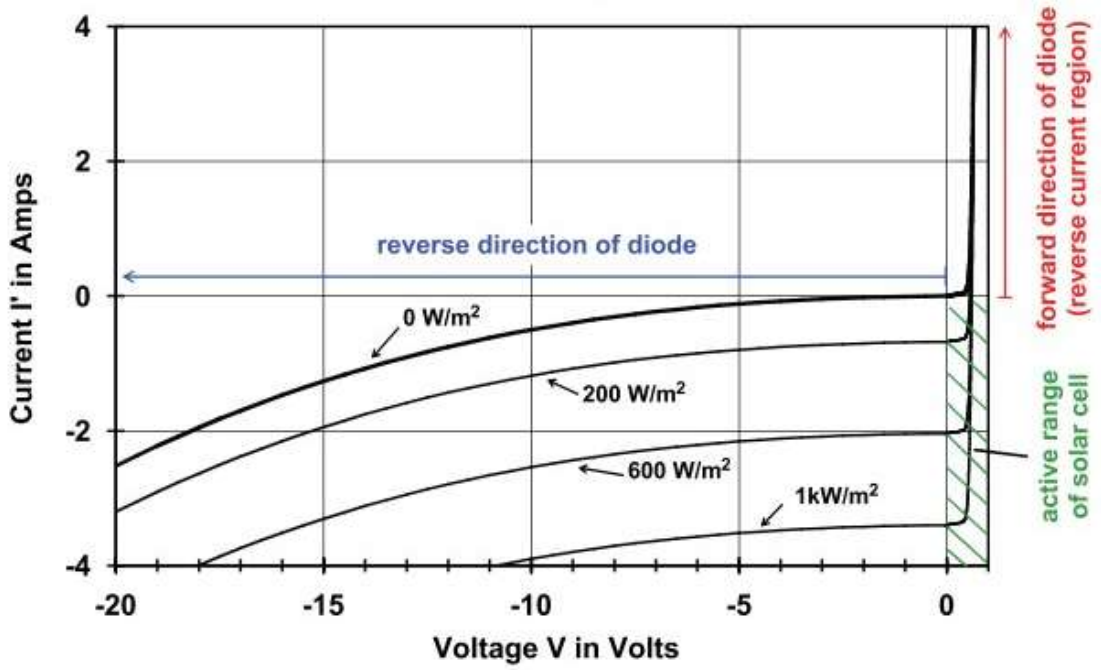

Figure 8. Characteristics of a Solar cell (monocrystalline, illuminated and dark) [4]

When in a series connection of PV cells one cell gets shaded, the voltage of that cell becomes negative. The shaded cell is now subject to the voltage produced by the non-shaded cells which can result in a hot spot in the PV cell that is shaded. As a counter-measure to this phenomenon bypass diodes are used. How they are connected is visible in figure 9. These diodes make sure that the current can flow through another path than the solar cell that is shaded. In practice only one bypass diode is used for a series connection of 12-24 solar cells.

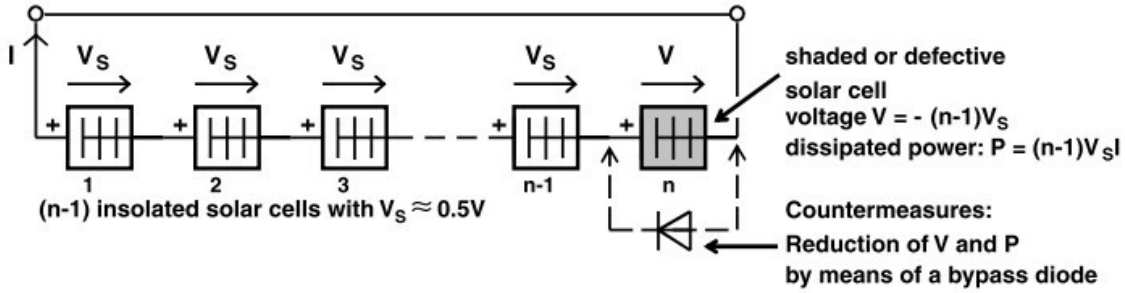

Figure 9. Principal of using bypass diodes in a series connection of PV modules. [4]

2.2.4 Partial shading and mismatch losses

Mismatch losses can be defined as the difference between the sum of the maximum power outputs of individual modules and the output of the system. As stated before when looking into the series connection of three PV-panels, there can be a global MPP and a local MPP. These multiple MPP's occur mostly when there is partial shading or unequal irradiation or temperature. From the moment one or more panels gets shaded, there will be some mismatch losses. It is the difference between the system maximum power and the sum of maximum powers of individual PV modules.

In figure 10 it is visible what the voltage-current curve is if the shaded panel has an irradiation of 400 W/m² and the unshaded panels 1000 W/m². In the series connection (purple curve) there is a voltage drop compared to the 3 panels of 1000 W/m² in series (red curve). This is because the bypass diode that is in use in the series connection has a little voltage drop over it. This voltage drop is also visible in the V_{OC} or the open circuit voltage between the series connection (purple curve) and the unshaded series connection (blue curve).

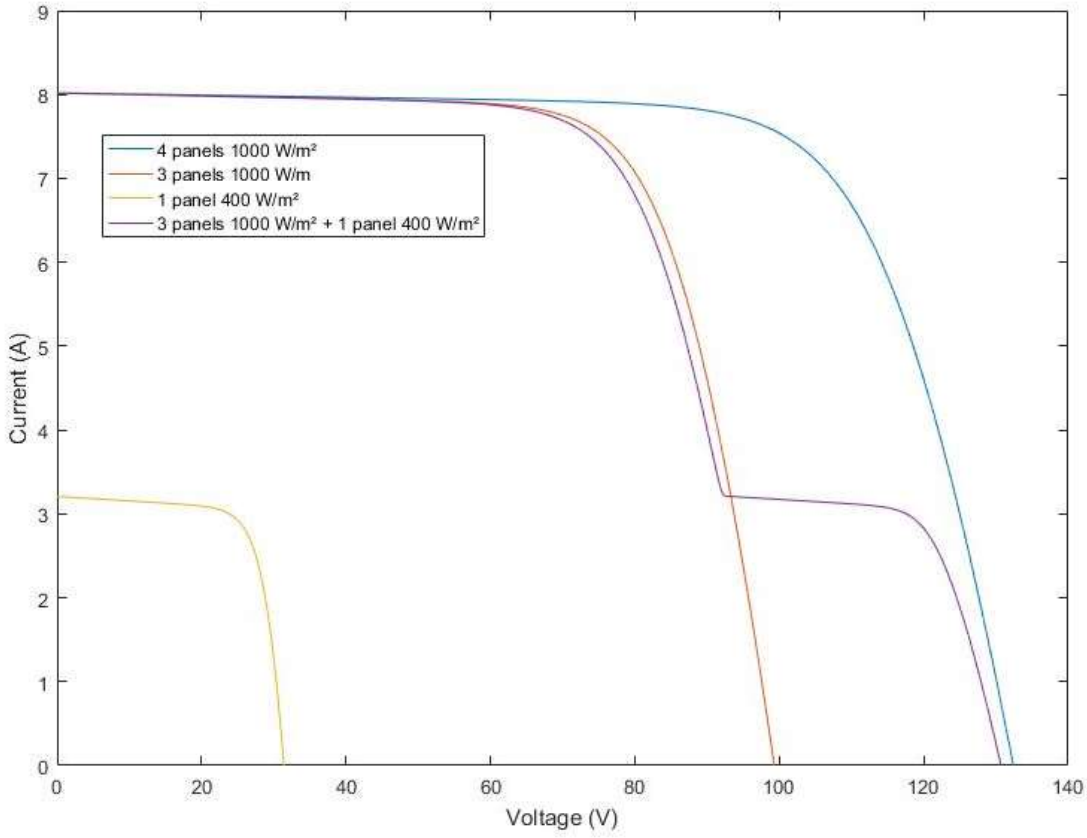

Figure 10. Voltage-current curve for a series connection of 3 PV modules with an irradiation of 1000 W/m² and 1 PV module with an irradiation of 400 W/m² (purple curve). The blue curve is the plot that shows the result when none of the panels are shaded. The red curve represents 3 unshaded panels while the yellow curve simulated one shaded PV panel.

To calculate the mismatch losses, it is mandatory to take a closer look at the voltage-power curves of this setup. These curves are presented in figure 11. The global MPP of the installation with one panel shaded is situated around 78 V. There is also a local MPP at 120 V with less power output than the global MPP. If the irradiation of the shaded panel would only differ a small amount from an unshaded panel then there would not be two MPP's, only a step would be visible in the curve instead of a local MPP like there is in this case. The partially shaded installation has a power output of 556 W in the global MPP. Compared to the power output of the unshaded installation which is 760 W, we see a power drop of 210 W or 25%. In theory the maximum power output is 643 W, this value is received by summing the power output from the shaded panel (73 W) with the power

output of the unshaded panels (570 W). So the mismatch losses are around 87 W or 13.5%.

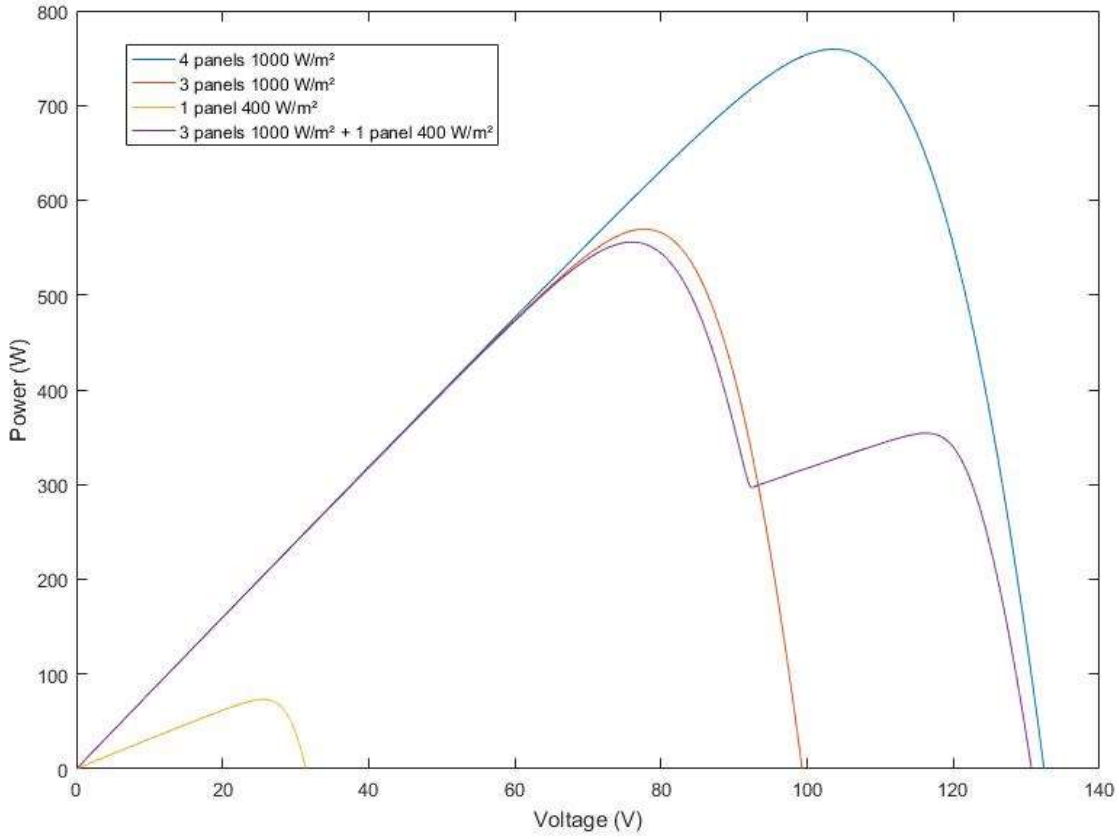

Figure 11. Voltage-power curve for a series connection of 3 PV modules with an irradiation of 1000 W/m² and 1 PV module with an irradiation of 400 W/m (purple curve)². Yellow curve represents one shaded panel with 400 W/m² irradiance. The blue curve represents 4 series connected panels with 1000 W/m². Red curve is 3 panels in series at 1000 W/m².

2.2.5 Influence of different operating conditions

For a photovoltaic cell the operating temperature is a value that varies a lot. Not only the ambient temperature but also the irradiance influences the operating temperature. The short-circuit current I_{sc} and the saturation current I_0 of a photovoltaic cell are not that much temperature dependant. I_0 is dependant of the temperature according to equation

$$I_0 = BT^{\gamma} e^{\frac{-E_{g0}}{kT}}, \tag{2.1}$$

where B is a constant that is temperature independent, E_{g0} is the zero temperature band gap energy of the semiconductor making up the cell that has been linearly extrapolated. The constant γ includes the temperature dependencies of the remaining parameter I_0. Some typical values for silicon are $E_{g0} \sim 1.2$ eV and $\gamma \sim 3$ [6]. B can be solved from equation (2.1).

$$I_{sc} = \frac{I_0}{T^{\gamma} e^{\frac{-E_{g0}}{kT}}} \tag{2.2}$$

When T is 25 °C and I_0 is 1.10^{-10} A then B has a value of about 726. For the one diode model illustrated in figure 20, the relation between the open-circuit voltage and the short-circuit current can be solved from equation (2.8) used further in this thesis, if we do not take the parasitic resistances into account, [6]

$$I_{sc} = I_0 \left(e^{\frac{qU_{oc}}{AkT}} - 1 \right). \tag{2.3}$$

If we neglect the small negative term, then the short-circuit current can be written as

$$I_{sc} = BT^{\gamma} e^{\frac{-E_{g0}}{kT}} e^{\frac{qU_{oc}}{AkT}} = BT^{\gamma}\, e^{\frac{qU_{oc}}{AkT} - \frac{E_{g0}}{kT}}. \tag{2.4}$$

Rearranging equation (2.4) gives us

$$Uoc = \frac{AkT}{q}\, ln \frac{I_{sc}}{BT^{\gamma}} + \frac{AE_{g0}}{q} = \frac{A}{q}(kT\, ln \frac{I_{sc}}{BT^{\gamma}} + E_{g0)}\,. \tag{2.5}$$

For silicon photovoltaic cells, the temperature coefficient of the open-circuit voltage varies between -0.3 and -0.4 %/K. Because of this the open-circuit voltage will de-

crease as temperature increases with a value between 1.7 and 2.9 mV/K. Then the temperature coefficient for the short-circuit current is from 0.04 to 0.05 %/K. The SC current increases as the temperature rises because the band gap energy E_g decreases and photons with less energy are able to create electron-hole pairs. The power output of the PV cell decreases when the temperature increases, by around 0.4 to 0.5 %/K. [6]

The influence of the temperature is examined by taking the a constant value for the irradiation. The fixed irradiance for this simulation is 1000 W/m². The results, given in figure 12, give us the insight that there is a considerable power loss if the cell temperature gets too high. This because the V_{OC} drops when the cell temperature gets higher.

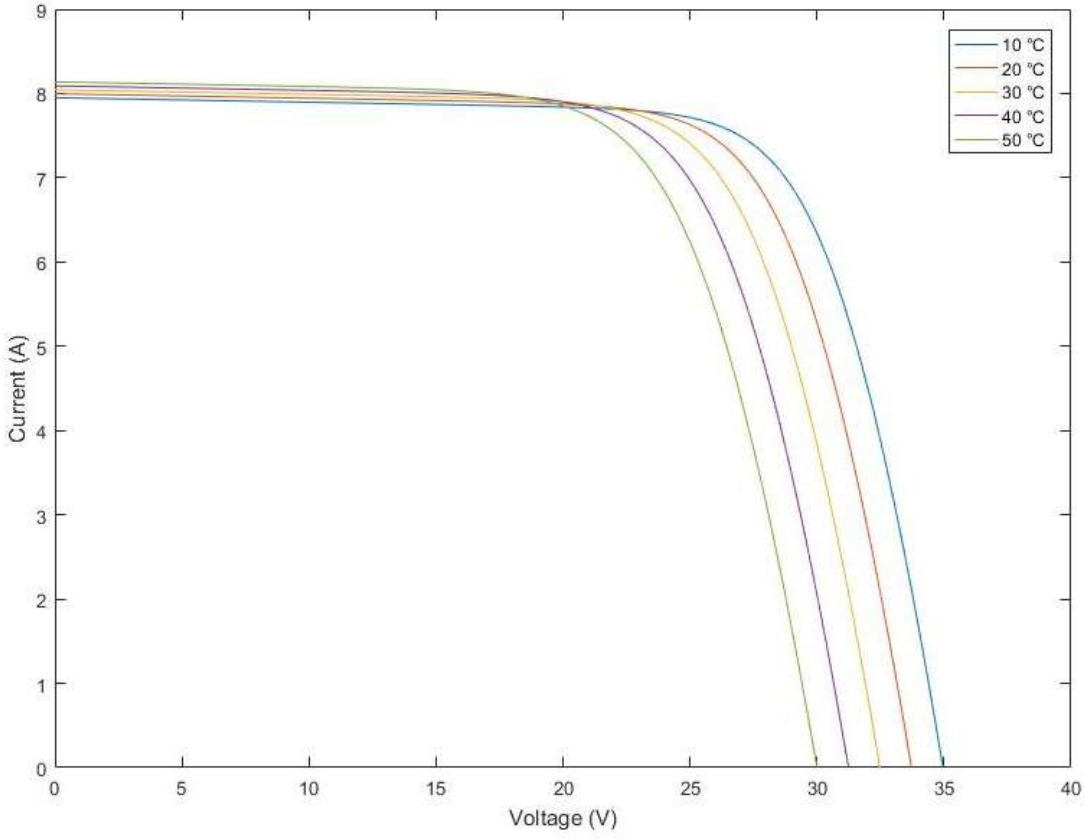

Figuur 12. Voltage-current curve for different values of module temperature with constant module irradiance.

To see how big the power losses are it is recommended to look at the voltage-power curves in figure 13. For 10 °C the power output for a single PV-panel is 203 W.

However , for a PV panel at 50 °C the power output is only 167 W. The increased temperature has induced a power drop of 17%. The influence of the temperature with constant irradiance on the voltage-power curve is shown in figure 13.

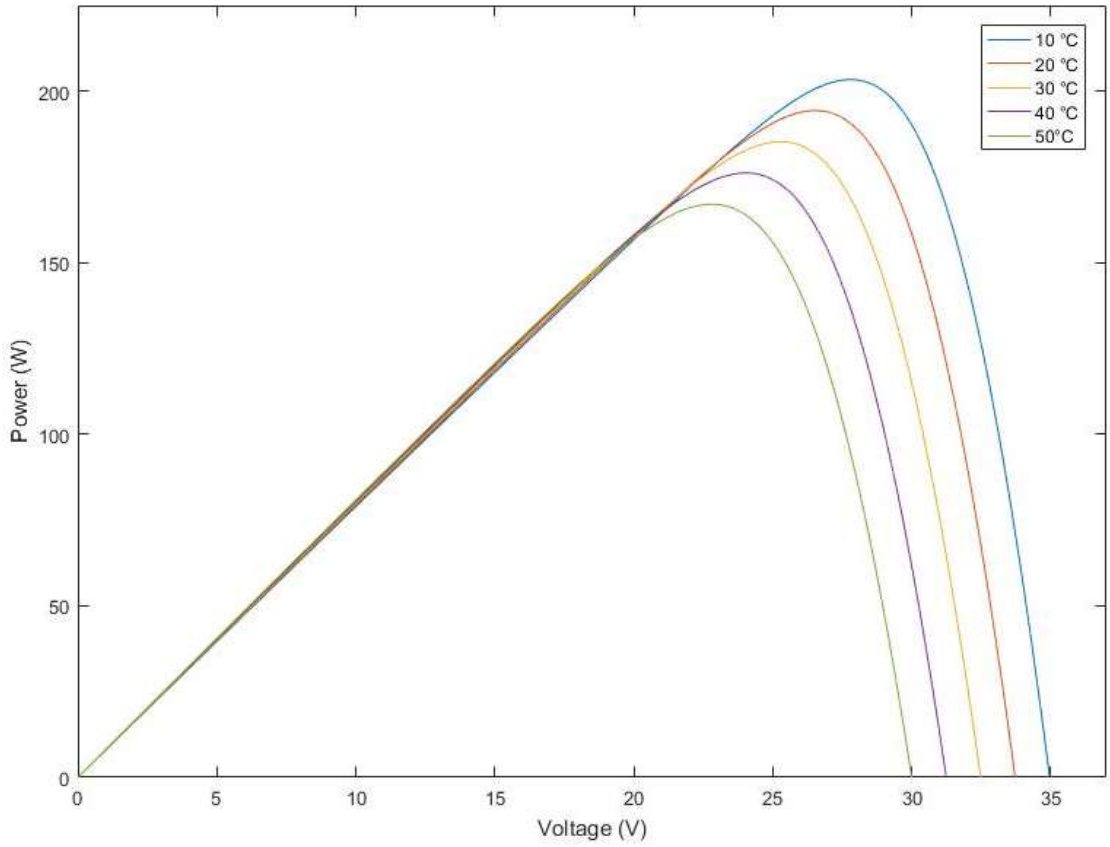

Figure 13. Voltage-power curves for different values of module temperature with constant module irradiance of 1000 W/m².

For the next simulation the cell temperature for each irradiance is fixed at 25 °C and irradiance is varied in figure 14. In reality when the irradiance gets higher it means that there is more sunlight insolating the panel and the temperature would rise as well. This phenomenon can be estimated with equation

$$T_{\text{cell}} = T_{\text{amb}} + K_{\text{T}}G, \tag{2.6}$$

where K_T is the temperature-rise coefficient. It is hard to perfectly determine the value of K_T but it is usually done through measurements using equation

$$K_{\mathrm{T}} = \frac{T_{\mathrm{cell}} - T_{\mathrm{amb}}}{G}. \tag{2.7}$$

This value is only a good estimation when measured during typical weather conditions. The temperature-rise coefficient for a typical PV module varies between 0.015 and 0.035 K/W/m². [6]

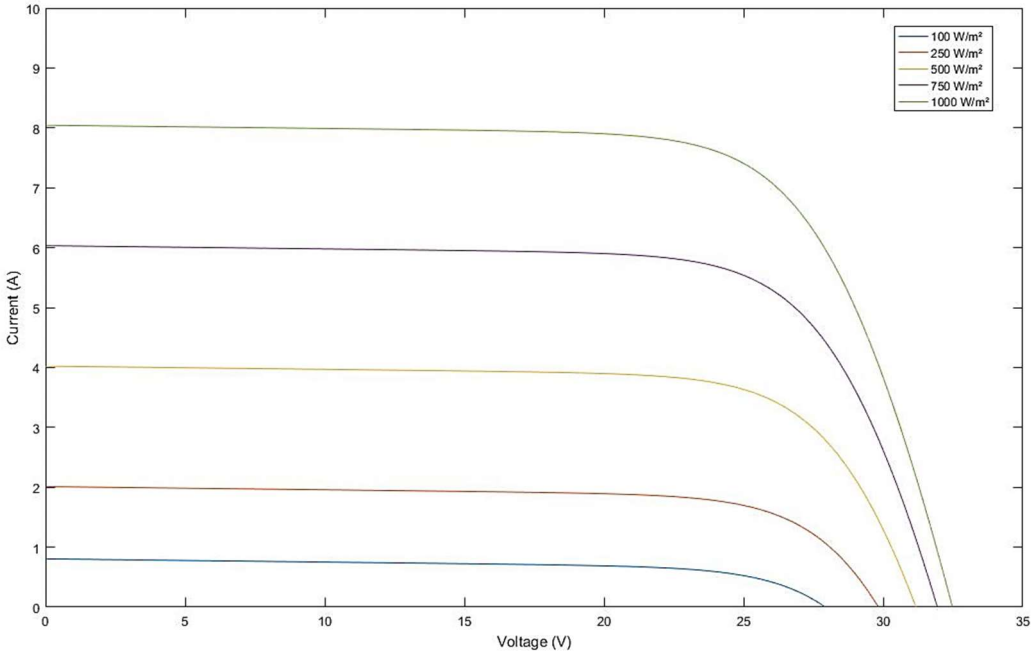

Figure 14. Voltage-current curves for different values of irradiance with constant module temperature of 25 °C.

The light-generated current I_{ph} is proportional to the flux of photons who create electron-hole pairs and the flux of photons is proportional to the incident irradiance. Therefore, the short-circuit current is directly proportional to the irradiance reaching the PV-panel. However, the influence of the irradiance on the open-circuit voltage is much smaller as can be seen on the figures. The OC-voltage (open-circuit voltage) at 100 W/m² is around 27.5 V and at 1000 W/m² the OC-voltage is increased to 32.5 V.

The short circuit current is directly proportional to the irradiance. The open-circuit voltage depends on the short-circuit current and, therefore, on the irradiance. This can be proven with equation (2.8).

$$V_{OC} = \frac{kT}{q} \ln \frac{I_{SC} + I_{01}}{I_{01}} = \frac{kT}{q} \ln(\frac{I_{SC}}{I_{01}}), \quad (2.8)$$

When $I_{SC} >> I_{01}$.

V_{oc} is the open circuit voltage of the PV installation. The other symbols used in this equation are explained in 2.2.7 *Modelling of a PV module*.

In figure 15 the voltage-power curve is presented for the case where the module temperature is constant and the irradiance varies. If there is more irradiance on the PV module then the power output of the module increases. With higher irradiances the OC-voltage increases slightly as well. What is also visible in figure 15 is the increasing maximum power point voltage with increasing irradiance.

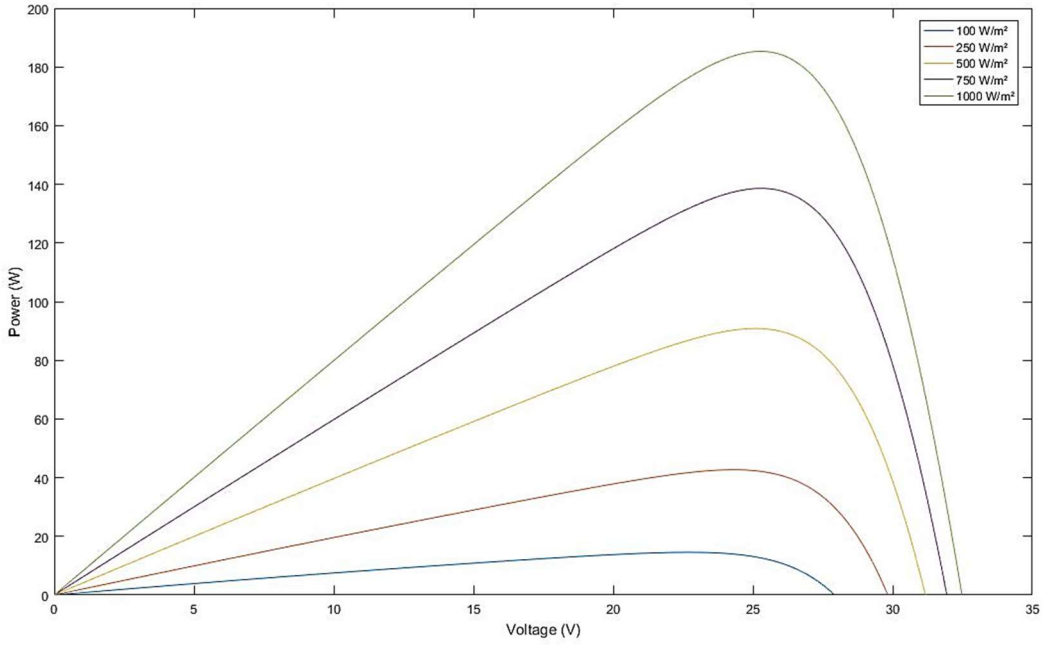

Figure 15. Voltage-power curves for different values of irradiance with constant module temperature of 25 °C.

2.2.6 Modelling of PV-module

Photovoltaic cells can be characterized by the current I and the voltage V if you consider them to be ideal.

$$I = I_{\mathrm{sc}} - I_{01}\left(e^{\frac{qV}{kT}} - 1\right) - I_{02}\left(e^{\frac{qV}{2kT}} - 1\right) \tag{2.9}$$

I_{sc} is the short-circuit current, I_{01} and I_{02} are the dark saturation currents. For these parameters experimental values are used or values given by the manufacturer of the photovoltaic cells. The temperature is given by T , the elementary charge by q and the constant k used in the equation is known as the Boltzmann constant. This equation is easily representable in the circuit diagram of figure 18.

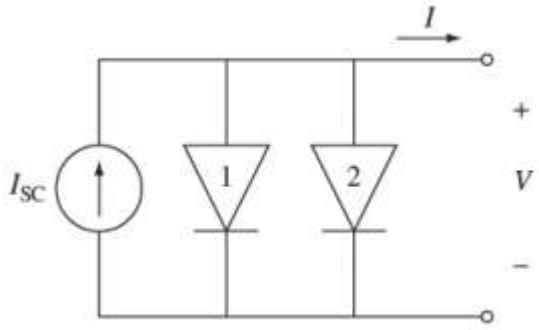

Figure 18. Diagram representation of equation (2.9) [12]

This ideal photovoltaic cell is useful to understand the basic working mechanism. However this does not represent the real photovoltaic cells. For this we need to add the parasitic resistances to the model. Adding the parasitic resistances to the equation gives a new equation.

$$I = I'_{\mathrm{sc}} - I_{01}\left(e^{\frac{q(V+IR_s)}{kT}} - 1\right) - I_{02}\left(e^{\frac{q(V+IR_s)}{2kT}} - 1\right) - (V + IR_{\mathrm{s}})/R_{\mathrm{sh}}, \tag{2.10}$$

where I'_{sc} is the short-circuit current without parasitic resistances, R_s is the series resistance and R_{sh} represents the shunt resistance. From this equation the diagram in figure 19 can be constructed.

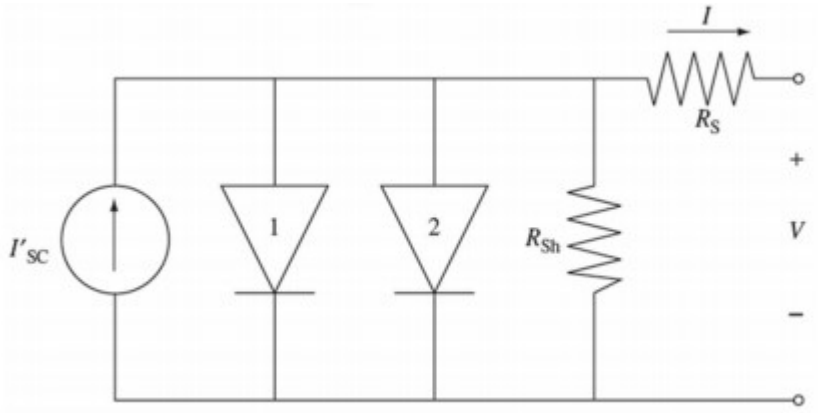

Figure 19. Diagram representation of equation (2.10) [12]

We can assume that dark saturations current of the quasi-neutral region dominate in the cell. This way we can simplify the model by combining the two diodes into one diode. This brings us to the one-diode model of a PV cell, seen in figure 20, which is common known and used in various articles.

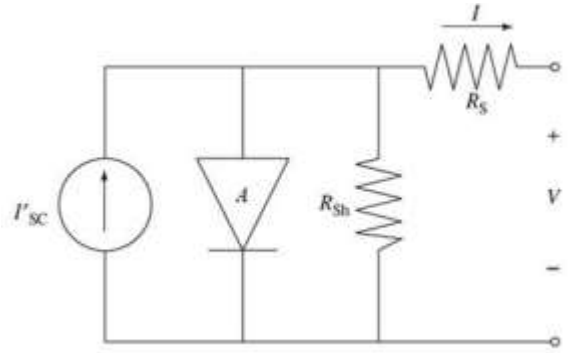

Figure20. Single diode model of a photovoltaic cell, represents equation (2.11) [12]

From this model a new equation can be formulated.

$$I = I'_{\mathrm{sc}} - I_0\left(e^{\frac{q(V+IR_s)}{AkT}} - 1\right) - (V + IR_{\mathrm{s}})/R_{\mathrm{sh}} \tag{2.11}$$

Because we combined the two diodes we need to introduce the ideality factor *A* to consider both dark saturation currents. The value depends on the type, material and structure of the PV cell and varies between 1 and 2. The main factors that influence the power output are the irradiance that reaches the surface of the cell and the temperature at which the cell operates. This can be simulated with our single diode model in Matlab. The results will be discussed further on in this thesis. The deductions made in chapter 2 are based on information obtained from *Photovoltaics System Design and Practice* by Heinrich Häberlin and the lectures of Seppo Valkealahti. [4] [12]

3. PV GENERATOR MODEL, SIMULATION MODEL AND SYSTEM SETUP

3.1 Simulink models

In this subchapter the used Simulink models that simulate the PV generator will be discussed. These models were created by Kari Lappalainen and are now used for more specific simulations concerning shadows caused by buildings in this thesis. The simulations were done with the single diode model. The differences between the model with ambient temperature is handled in chapter 4 where the results are presented.

3.1.1 Single diode model

In Matlab, the single diode model made by Kari Lappalainen is used. The parametrization of this model has already been done and checked. This model is given in figure 21. [6]

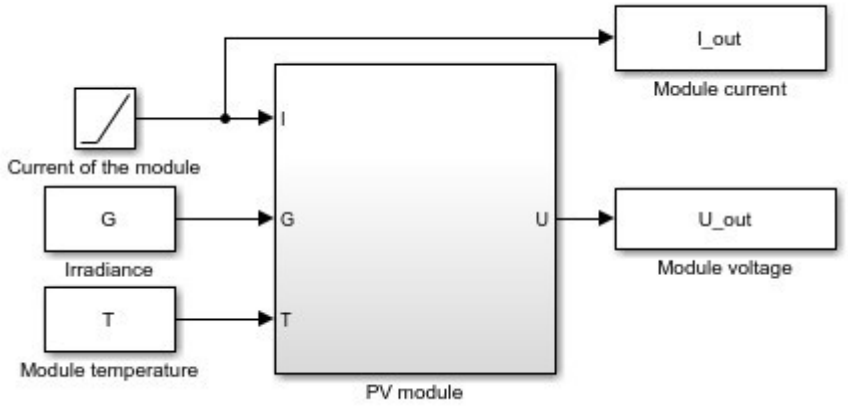

Figure 21. Single diode model used in Simulink for the simulations in this thesis. [6]

The input parameters are the temperature *T* and the irradiance *G* of the PV-module. As a result you get the produced voltage *U_out* and current *I_out*. In this thesis we often

use *V* for the produced voltage and *I* for the produced current. In the models however the symbols *U_out* and *I_out* are used. With basic math operations it is possible to calculate the produced power and mismatch losses with these parameters. Opening the PV module in Simulink gives the following model in figure 22.

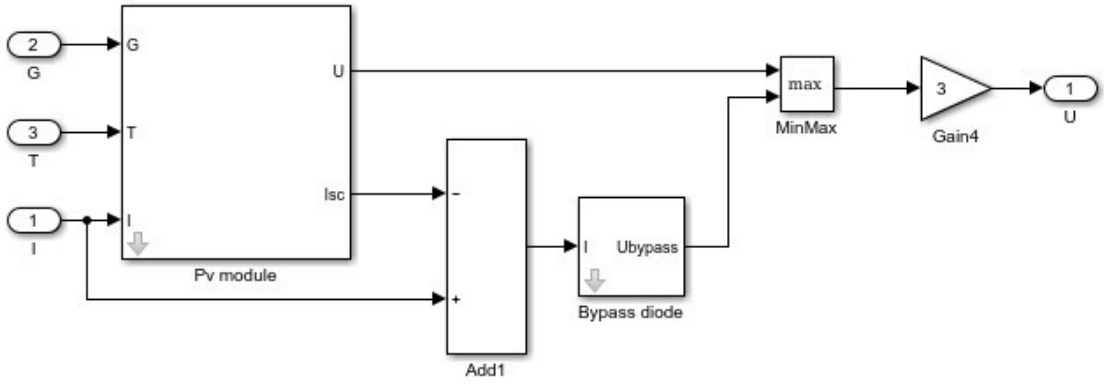

Figure 22. This is the Simulink model of the "PV module" in figure 18. [6]

This model basically reproduces the equation of the single diode model. The value of the produced voltage *U_out* is isolated from the equation which leads to this setup of the model.

3.2 Characteristics of PV panel

The used PV modules in the studied system setup, which is described more detailed in subchapter 3.3, are the NAPS NP190GKg PV modules. The measured data that is used later in the thesis origins from the PV installation on the roof of the department of Electrical Engineering of Tampere University of Technology. That installation is made of 69 of these PV modules. The modules are made from multicrystalline Si PV cells. In each module there are 3 substrings of 18 PV cells with a total of 54 cells. The substrings are protected by bypass diodes. The simulations in this thesis can differ slightly if other PV models were used. The parameters provided by the manufacturer for the NAPS NP190GKg PV module are presented in Table 3.1.

Table 3.1. Parameters for the NAPS NP190GKg PV module in Standard Testing Conditions (STC). [6]

Parameter	*Value*
$I_{SC,STC}$	8.02 A
$U_{OC,STC}$	33.1 V
$P_{MPP,STC}$	190 W
$I_{MPP,STC}$	7.33 A
$U_{MPP,STC}$	25.9 V
N_s	54

Different parameters had to be determined to use the Simulink models for simulations. These parameters are presented in Table 3.2. To determine the series and shunt resistance of the PV module, the aforepresented method was used. For Si PV cells an ideality factor of 1.30 is used which is a typical value for these sort of PV cells. The current and voltage temperature coefficients K_I an K_U are received from chapter 2.2.5 where the effect of temperature is represented. Measured values of temperature and irradiance are used to estimate the temperature-rise coefficient by using equation (2.7).

Table 3.2. Parameters for the NAPS NP190GKg PV module that is used in the simulations. [6]

Parameter	*Value*
R_s	0.3294 Ω
R_{sh}	187.8790 Ω
A	1.30
K_I	0.0047 A/K
K_U	-0.1240 V/K
K_T	0.0325 K/W/m²

For the bypass diodes the parameters are presented in Table 3.3. It is assumed that the temperature of the bypass diode is the same as the ambient temperature and thus constant. The ideality factor, series resistance and the saturation current are determined by curve fitting to the I-U curve of a Schottky diode. In the single diode model, the bypass diode is modelled so that when the current of the module is greater than the short-circuit current of the module, the bypass diode conducts. [6]

Table 3.3. Parameters for the bypass diodes that are also used in the Simulink simulations [6]

Parameter	*Value*
A_{bypass}	1.50
$R_{s,bypass}$	0.02 Ω
$I_{0,bypass}$	3.20 μA

The simulation models used in SIMULINK are a simplification of the reality. When the single diode model is used, the parasitic resistances remain constant and the losses in the cables are neglected. Furthermore the irradiance, and thus the temperature, is not equal for the whole PV panel. Also, all the PV modules that are connected in the installation are not perfectly equal to one another. A more detailed explanation of all the models used and the parametrization of these models can be found in Kari Lappalainen's *Effects of Climate and Environmental Conditions on the Operation of Solar Photovoltaic Generators*. [6]

3.3 Studied system setup

The used system setup is represented in figure 23. The photovoltaic array consists out of 18 PV panels connected in series. The characteristics of the PV panel are discussed in subchapter 3.5. The length of one PV panel is 1.475 m. Each panel has three bypass diodes. When the shadow hits a panel in the PV array, this panel will receive only 10% of the irradiance. This is the amount of diffuse irradiance that is insolating the shadow

part of the panel. Because of the geometry and connection of the photovoltaic cells in the panel, the total output current will be limited to the lowest output current that is present. The shaded cells of the PV panel will produce this low current. [12]

In the simulation program the assumption is made that the shadow passes over the array in a perpendicular way to the PV-string. Also the height of the building is chosen high enough so that the PV-array is always completely covered in shadow in the vertical direction.

In this first case the object causing shadow is 40 m long while the PV-array is 18 panels long (26.55 m). The distance between the PV-array and the object causing the shadow is set at 50 m. When the sun moves from the right to the left, there are two corners of the object that have to be taken into account. These corners define the shadow of the object.

With basic geometry the angles Θ_1 and Θ_2 can be found. The first angle Θ_1 has a value of 0.9836 radians (56.36 °), Θ_2 has the value of 1.4371 radians (82.34 °). Between these angles the PV array goes from fully unshaded to fully shaded. With the angular velocity of the sun equal to $7 \cdot 10^{-5}$ rad/s it is possible to calculate the necessary time for that.

Matlab is a program that works with arrays and lists. To work efficiently it is recommended to choose a certain time step. In this case a timestep of 10 seconds has been chosen. For this amount of time the shadow has moved $7 \cdot 10^{-4}$ radians (0.04 °) which matches a certain amount of distance travelled by the shadow edge. The average amount is around 0.045 m for each timestep of 10 sec. Every time this distance reaches a multiple of the length of a PV panel (1.475 m), the next panel in the series connected PV-panels will receive only 10% of the irradiance.

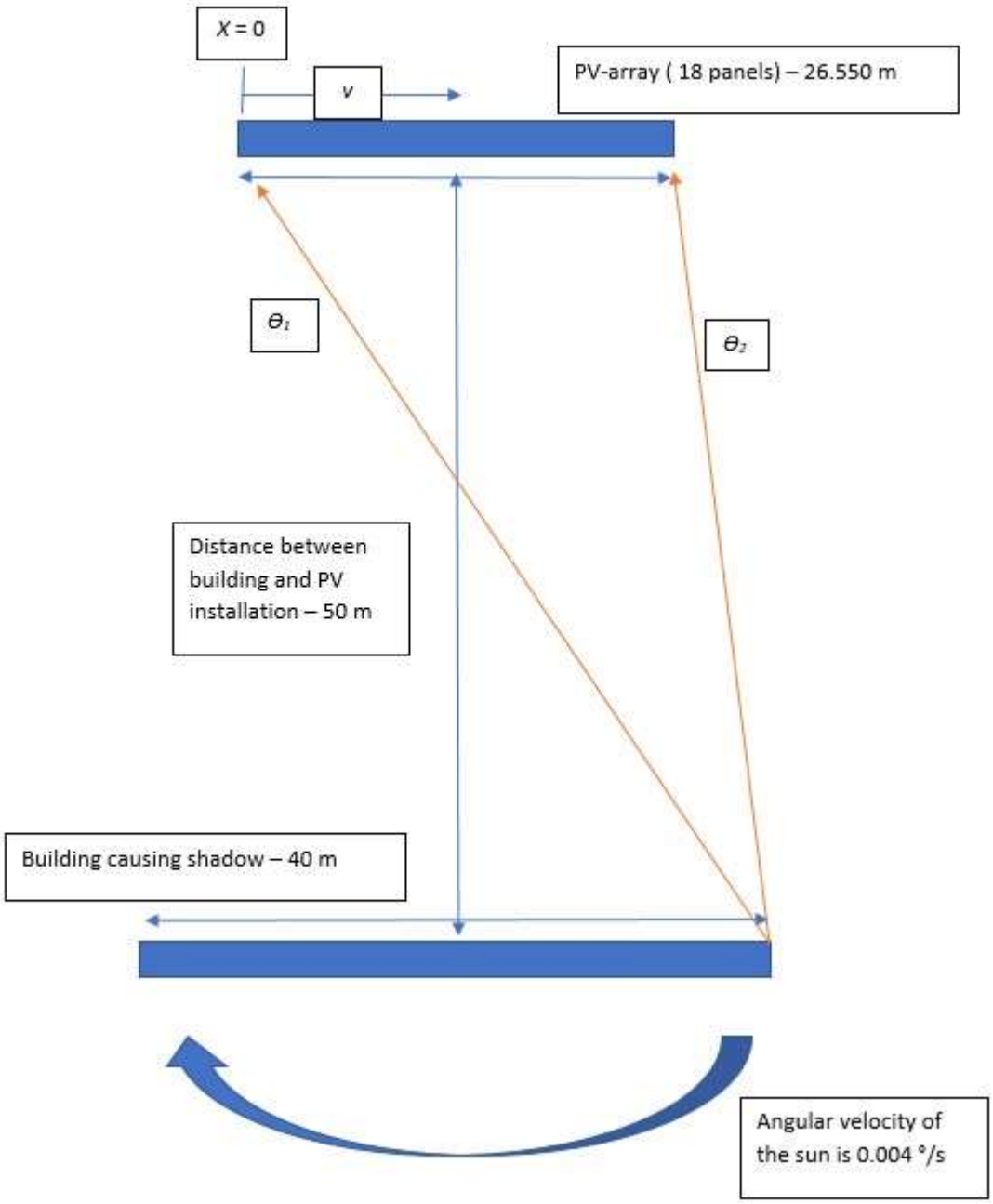

Figure 23. The studied system setup.

3.4 Necessary system setup parameters

To fluently use the program, some parameters can be calculated in advance. To make the program not too complex it is recommended to use a constant value for the angular velocity of the sun. The speed with which the shadow moves over the PV installation is not constant in the horizontal direction. For this a formula needs to be derived.

3.4.1 Angular velocity of the sun

To know how fast the shadow passes over the PV-string, we need to know the angular velocity of the sun during the day. If the heading in degrees is know where the sun rises and where the sun sets, we know the angle the sun has made during that day. By looking at the time when the sun rises and sets we know how long the sun needed to complete a full day of sunlight. With these 4 parameters we can calculate the angular velocity.

For example when the sun rises at 07:26 with an angle of 104 ° and sets at 17:49 with an angle of 256 °, the sun travelled 2.65 radians in a time of 37380 seconds or 623 minutes that day. Since the distance and the time travelled are known the angular velocity can be calculated. For this specific day the angular velocity is $7.09 \cdot 10^{-5}$ rad/s (0.22 °/min). This angular speed varies throughout the year from $6.52 \cdot 10^{-5}$ rad/s minimum in the winter months to a value of $7.44 \cdot 10^{-5}$ rad/s (0.25 °/min) in the summer. To make this not too complex we will use the mean of 7 rad/s (0.24 °/min) as the angular velocity of the sun. This value can easily be changed in the simulation but won't have big effects on the results. It is obvious that this calculation of the angular velocity is not accurate but it's approximation is good enough to estimate the speed of the shadow passing over the PV-string. In figure 24 the path of the sun can be seen for different times of the year. [11]

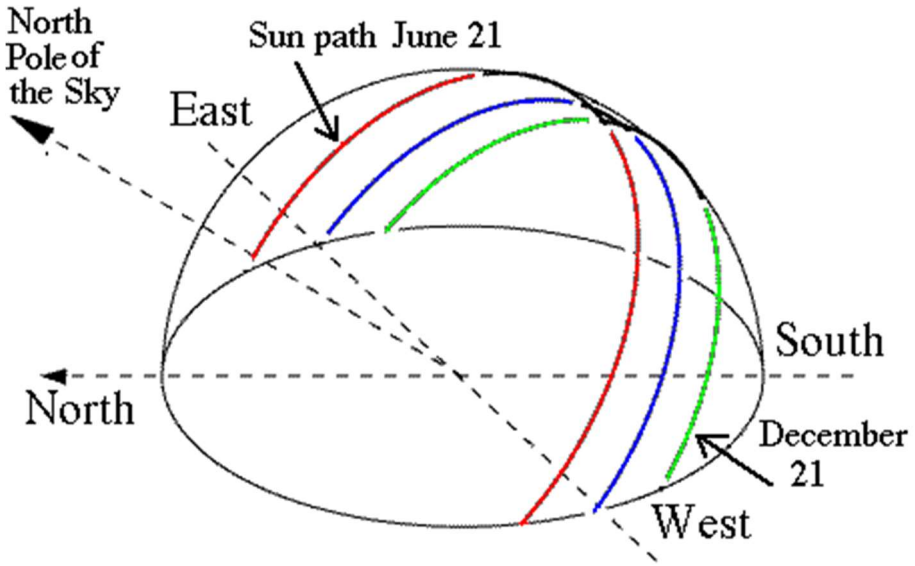

Figure 24. Sun paths for different times in the year. The angle that the sun makes on the horizontal circle is visible in the picture. [9]

3.4.2 Speed of the shadow

Basic geometry can lead us to a formula that gives us the speed of the shadow at any given time. The angle Θ is the angle mentioned in chapter 3.2 where the used system setup is presented. It is the angle between the direction of the orange arrows shown in figure 23 and the direction perpendicular to the position of the building that causes the shadow. The angle starts with a big value (Θ_1) when the shadow sets in the PV array from the left side. As the shadow continues moving to the right, the angle size declines until Θ_2.

$$tan\theta = \frac{x}{r} \tag{3.1}$$

$$r\,tan\theta = x \tag{3.2}$$

By differentiating equation (3.2) the next equation is obtained:

$$\frac{r}{cos^2\theta}\frac{d\theta}{dt} = \frac{dx}{dt} \tag{3.3}$$

$$\frac{r}{cos^2\theta}\ \omega = v. \tag{3.4}$$

The angular velocity ω, in equation (3.4), is that one of the sun. The radius r is the distance between the PV-array and the object causing the shadow. The angle Θ is shown on figure 23. The position of the shadow is characterized by *x* in the equations and in the program written in Matlab. The velocity of the shadow is *dx/dt* or *v*. The quantities *x* and *v* are also represented in figure 23.

Figure 25 shows us the relation between the angle Θ and the speed of the shadow that the object causes. This is the result for a certain setup (case 1) which is discussed later on. It is clear that if the angle is big then the shadow moves fastest over the PV-array. So the first PV panels in the array will be covered faster than the last one. This concept has to be taken into account when calculating the power output of this PV power generator.

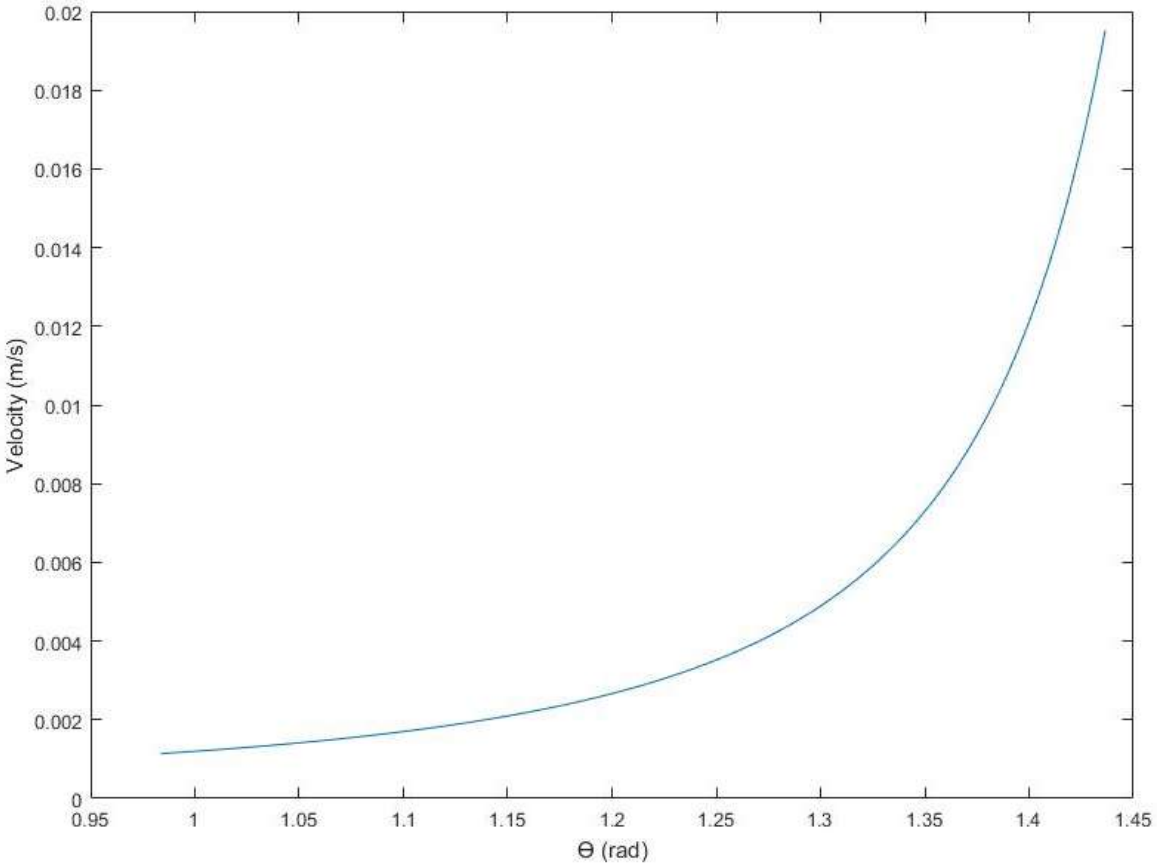

Figure 25. The velocity of the shadow on the PV array as a function of the angle Θ. The angle varies between 0.98 radians and 1.44 radians. For all the values in between the velocity is presented on the y-axis.

3.5 Simulation program

This paragraph will explain in short how the simulation program in this thesis is built up. To begin with there are several input parameters needed to calculate for the position of the shadow at any given time. Therefore the dimensions of the installation and the position relative to the object causing the shadow are mandatory. Afterwards the formula to calculate the speed of the shadow is implemented into the program. With this speed it is possible to pinpoint the exact location of the shadow. This position will be stored in an array called x. With $x = 0$ the edge of the shadow is in the beginning of the PV-installation and with $x = 26.55$ m it is in the end.

Since it is unnecessary to calculate these parameters each second, a timestep of 10 seconds is taken into account to calculate the position of the shadow. For some cases in this thesis a timestep of 100 seconds is used to make the program faster. That's why some graphs have only 500 timesteps while others have 5000. The size of the timesteps are important to take into account when calculating the total energy output of the PV-installation.

With the array *x*, the position of every new panel can be found every time a new multiplication of 1.475 m is found. This is the length of one PV-panel. Each time *x* reaches a value that is a multiplication of 1.475 m, another PV-panel is shaded. This can be explained with figure 26.

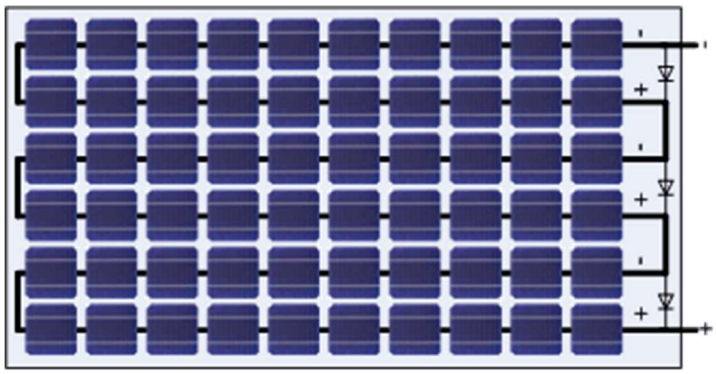

Figure 26. Solar panel – 60 cells connected as 3 strings of 20 with bypass diodes. [7]

When the shadow starts shading the left side of the panel, every serie connection of solar cells in the panel has a shaded solar cell. This cell blocks the current for the whole serie connection. The whole PV-panel is reduced to an irradiation equal to the shaded cells. Which is chosen to a value of 10% of the maximum irradiation. This 10% equals the amount of diffuse irradiation insolating the PV-panel.

The total power output of the system is then determined by the amount of panels shaded and the amount of them that are unshaded. For each situation the single diode model can be used to simulate the voltage and current outcome. This certain situation is valid for the amount of timesteps between two multiplication values of *x*. With the right mathematical operations, the mismatch losses and other necessary parameters can be calculated and plotted quite fast.

4. RESULTS

4.1 Fixed irradiation

In this subchapter the input for the single diode model is a fixed irradiation of 1000 W/m². This simulates the maximum power limit for the PV installation. In practice the sun in the beginning of the day and in the end of the day does not give it's full irradiation because the PV panels are inclined over a certain angle. These simulations give us the answer what potentially can be the power output if it the PV panels have a constant 1000 W/m² irradiation.

4.1.1 Voltage – current curves

When the shadow is at the first panel, the irradiance of the shaded part is only 10% of the full irradiance. In figure 27 the blue line represents the series connection between 17 unshaded PV panels and 1 shaded PV panel. This series connection is as good as equal to the curve of 17 unshaded PV panels, even at the highest voltages. There is only a small difference caused by the voltage drop of the bypass diode. The difference between the series connection and 18 unshaded PV panels is quite noticeable. In the voltage-power curve in figure 30 a power loss of around 5% is visible.

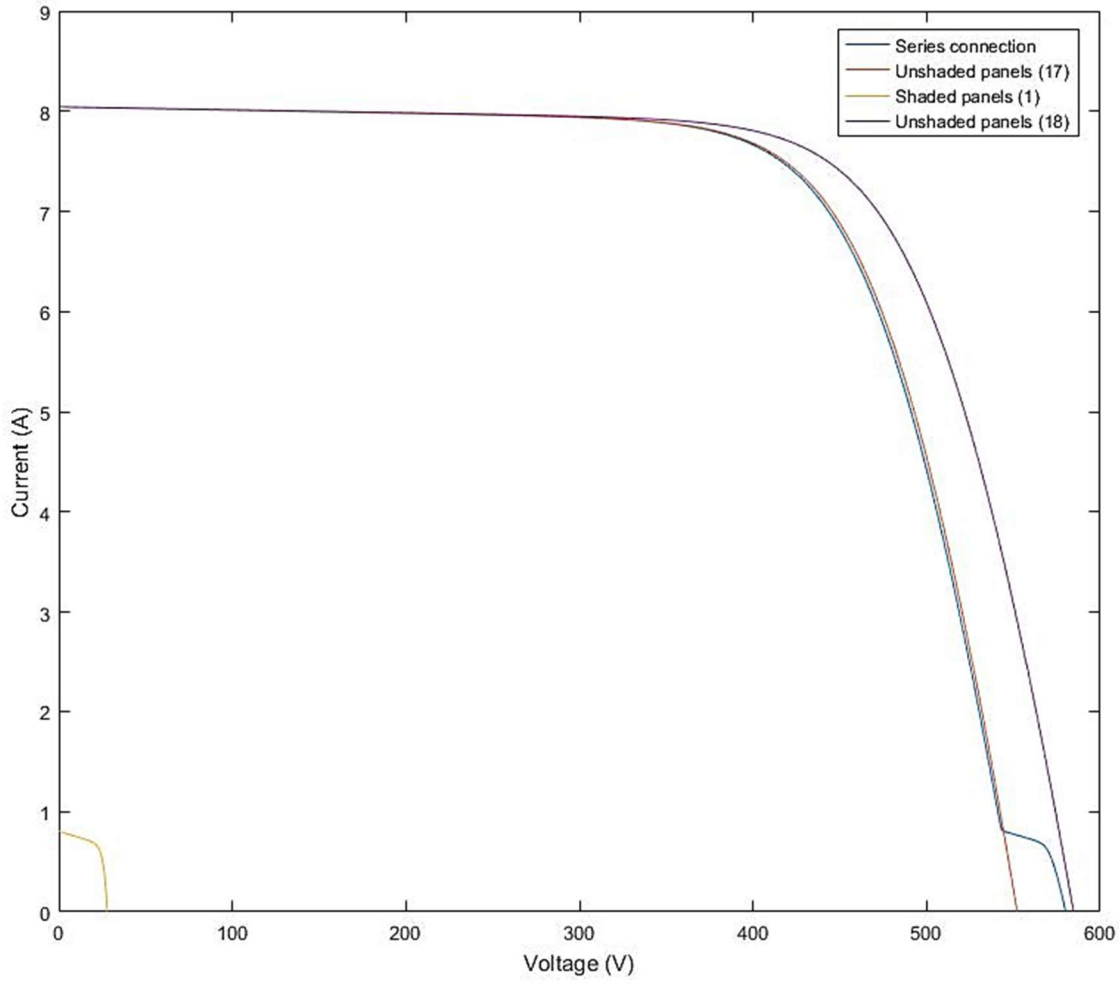

Figure 27. Voltage – current curve for series connection of 1 shaded panel and 17 unshaded panels. The shadow is located at the first panel of the array when it is assumed that it moves from left to right over the PV installation.

When the shadow reaches the ninth panel, half of the PV-array is shaded. This is clearly visible on the IV curve in figure 28. Half of the voltage is provided by the shaded panels which only deliver 10% of the unshaded panels current. The other half of the voltage is provided by the unshaded panels. The power losses when 9 PV panels are shaded is much bigger then when only 1 PV panel is shaded as in figure 27. The voltage drop between the series connection (blue curve) and the unshaded panels (red curve) is more visible then in figure 27 as well. This voltage drop is caused by the bypass diodes that are conducting the current when PV panels are shaded. If more panels get shaded then the cumulative voltage drop over the bypass diodes will rise as well.

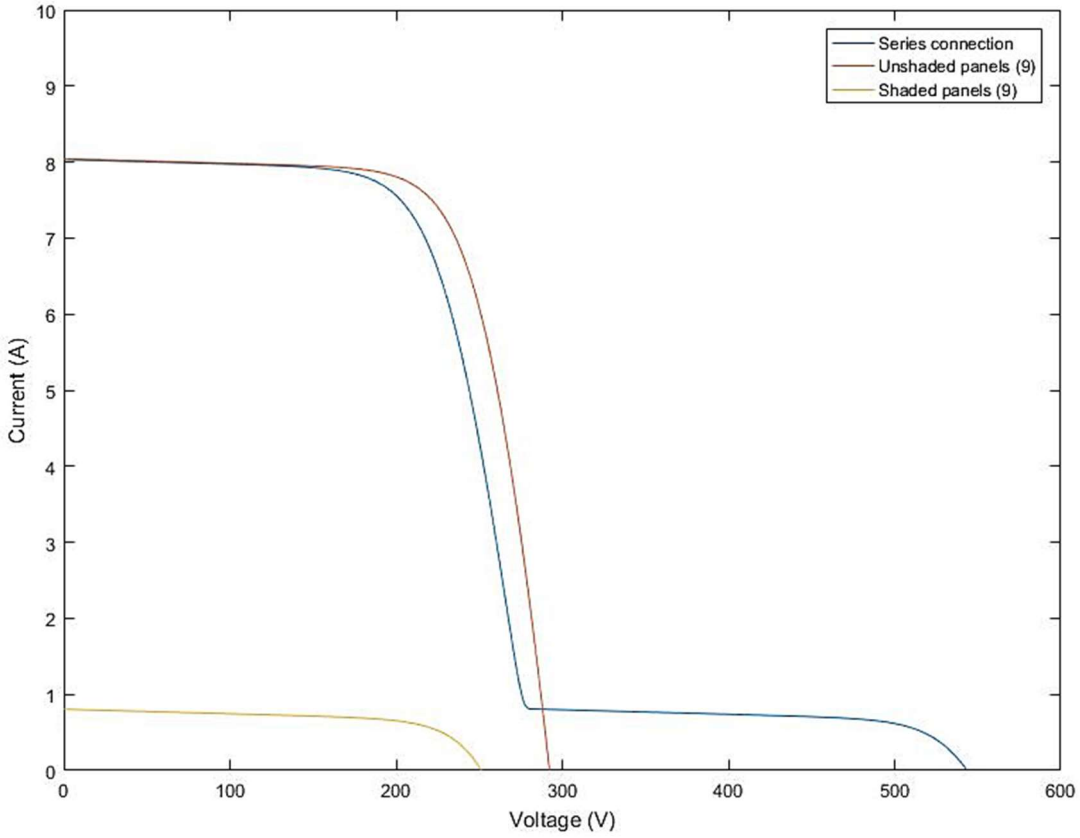

Figure 28. Voltage – current curve when the shadow is located at panel 9. This implies that this is a series connection of 9 unshaded PV panels and 9 shaded PV panels.

During the moment the shadow starts covering the last panel there are no unshaded panels left. There are only shaded panels who provide the power output. The overall current is limited to 10% in comparison with a normal 1000 W/m² irradiation. The voltage – current curve for this situation is drawn in figure 29. The open-circuit voltage is dropped with respect to 1000 W/m² irradiance since it decreases with decreasing irradiance, this has been proven in equation (2.8).

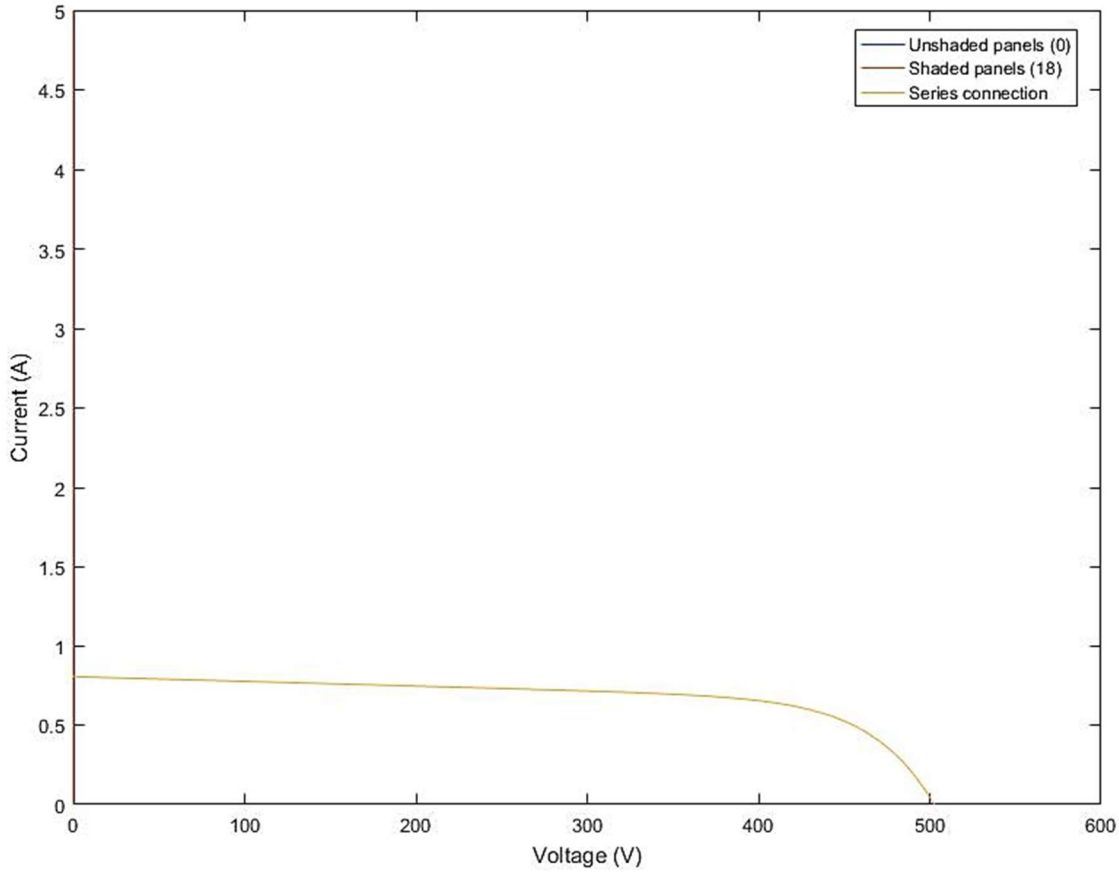

Figure 29. Voltage-current curve when the whole PV installation is covered by shadow caused by the building. Series connection of 18 shaded PV panels.

4.1.2 Voltage – power curves

When only the first panel is covered by the shadow, there is only a small power line visible from this shaded panel. This may not be completely clear in figure 30. The reason for this is that the available power for this single shaded panels is of the order of 14.5 W. Although in the total power curve given by figure 30, the influence of this shadow is more clearly visible. However, this bump in the total power curve does not cause a second MPP.

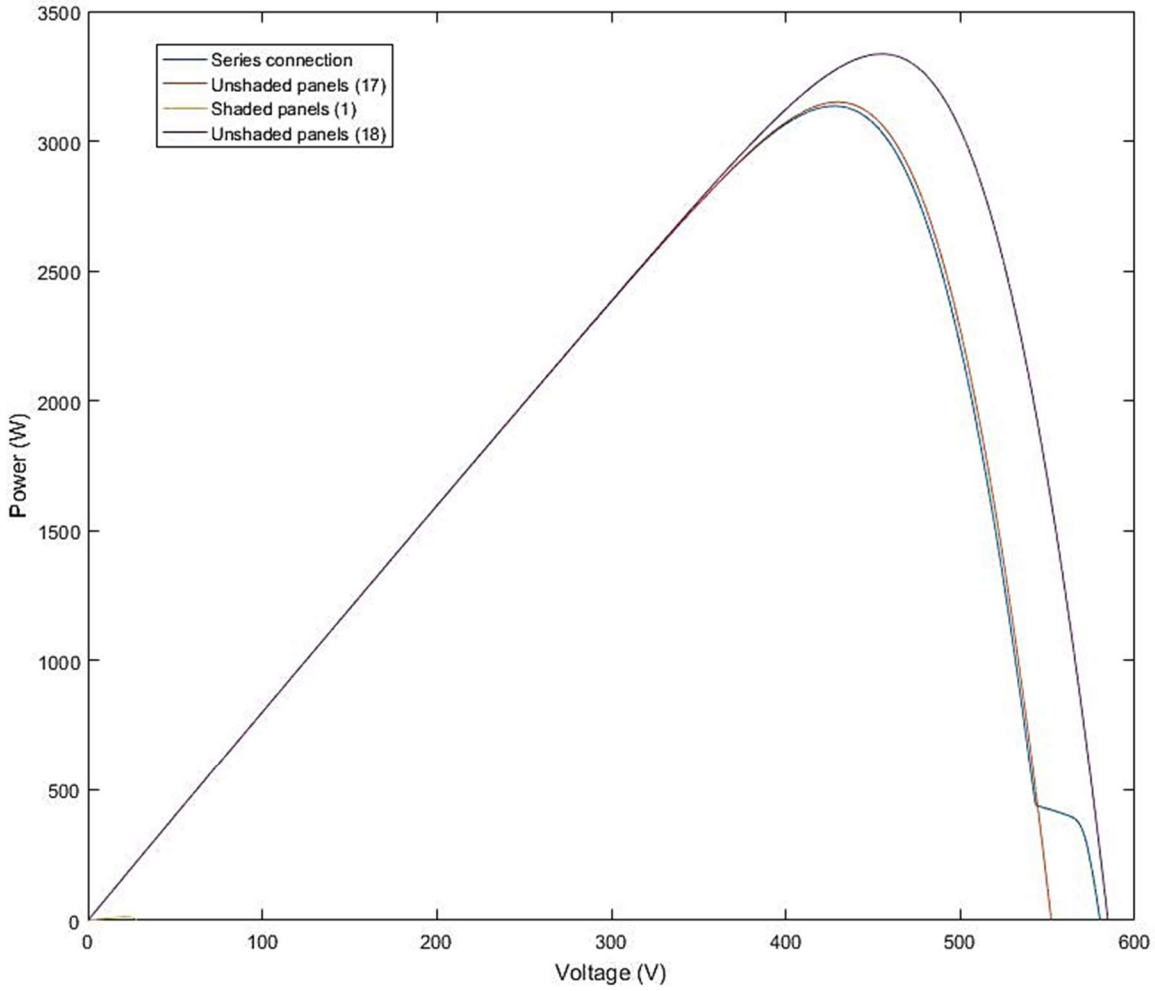

Figure 30. Voltage – power curve for series connection of 1 shaded panel and 17 unshaded panels. The shadow is located at the first panel of the array when it is assumed that it moves from left to right over the PV installation.

When the shadow is halfway the PV-string, the influence of the shaded panels is more clearly visible. In this case it is possible that the second MPP around 500 V can be seen as a local MPP. If the MMP tracking fails and follows the local MPP instead of the global one then this could lead to major power losses in the PV-installation. The voltage-power curve for this situation is given in figure 31.

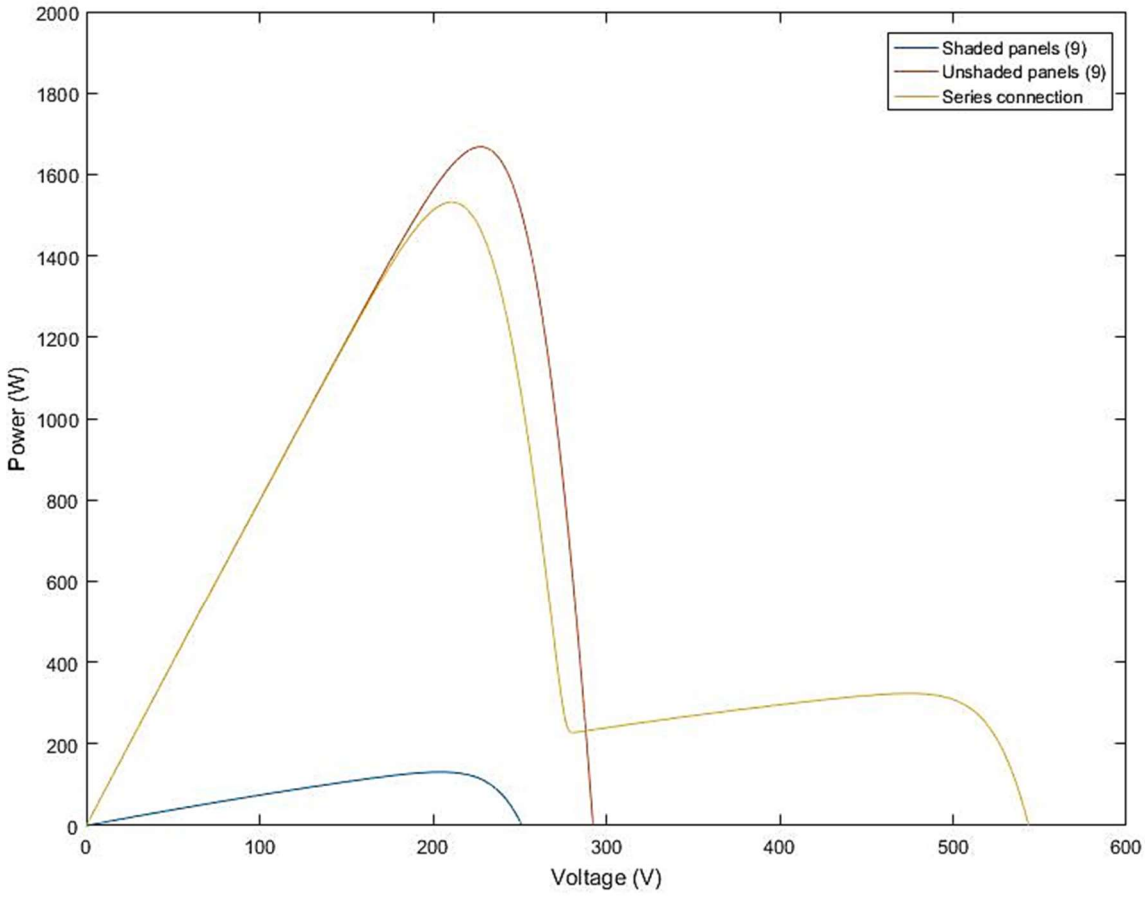

Figure 31. Voltage – power curve when the shadow edge is located at panel 9. This implies that this is a series connection (yellow curve) of 9 unshaded PV panels (red curve) and 9 shaded PV panels (blue curve).

When the shadow covers the whole installation, there is only around 10% power available from the power when the PV-string would work without shadow. Since there is no difference in irradiation for the PV-string, there is only one global MPP as visible in figure 32.

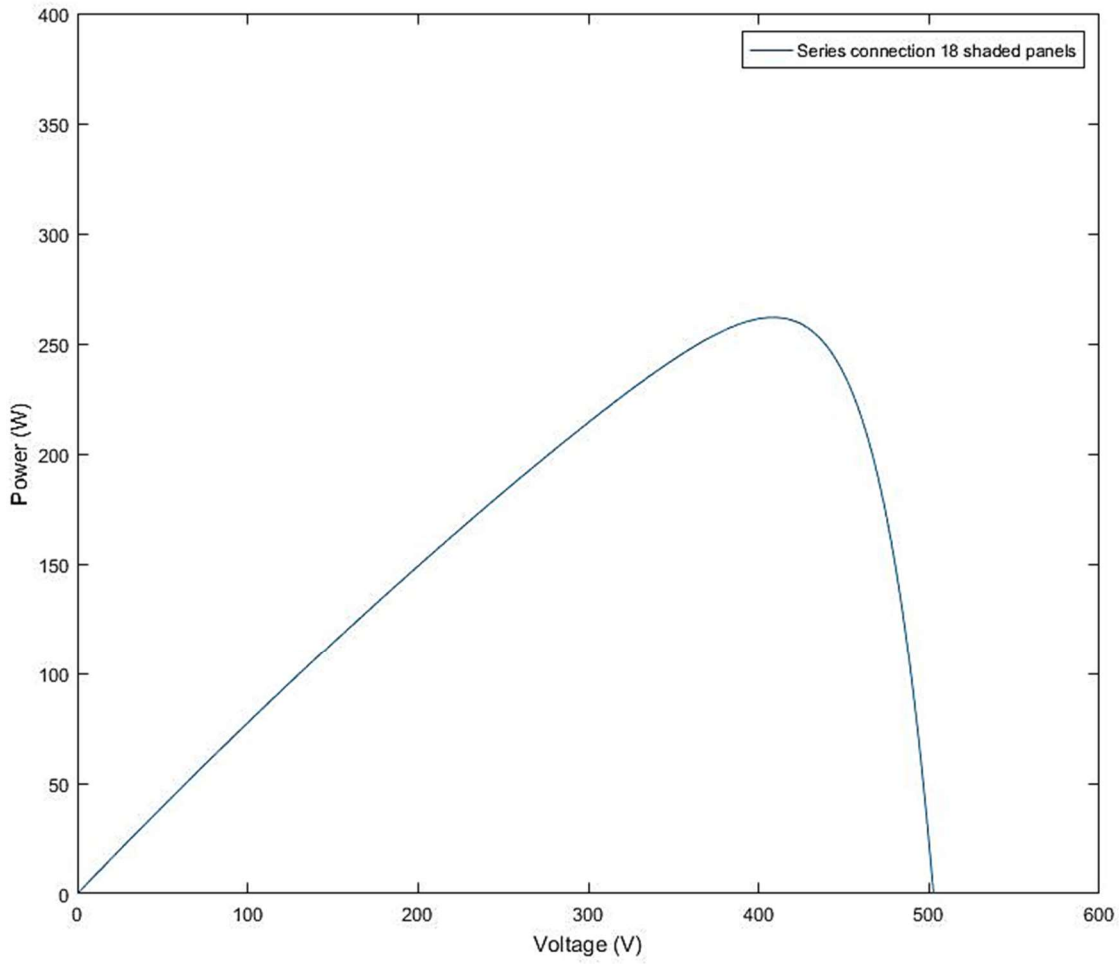

Figure 32. Voltage-power curve when the whole PV installation is covered by shadow caused by the building, i.e., a series connection of 18 shaded PV panels.

4.1.3 Mismatch losses

A first look at the mismatch losses gives us the logical outcome: the more panels are shaded the higher the mismatch losses are. The mismatch losses can be calculated as how much energy there is lost or how much power (figure 33). These mismatch losses are calculated for the system setup explained in 3.2. Figure 34 gives us the relative power loss.

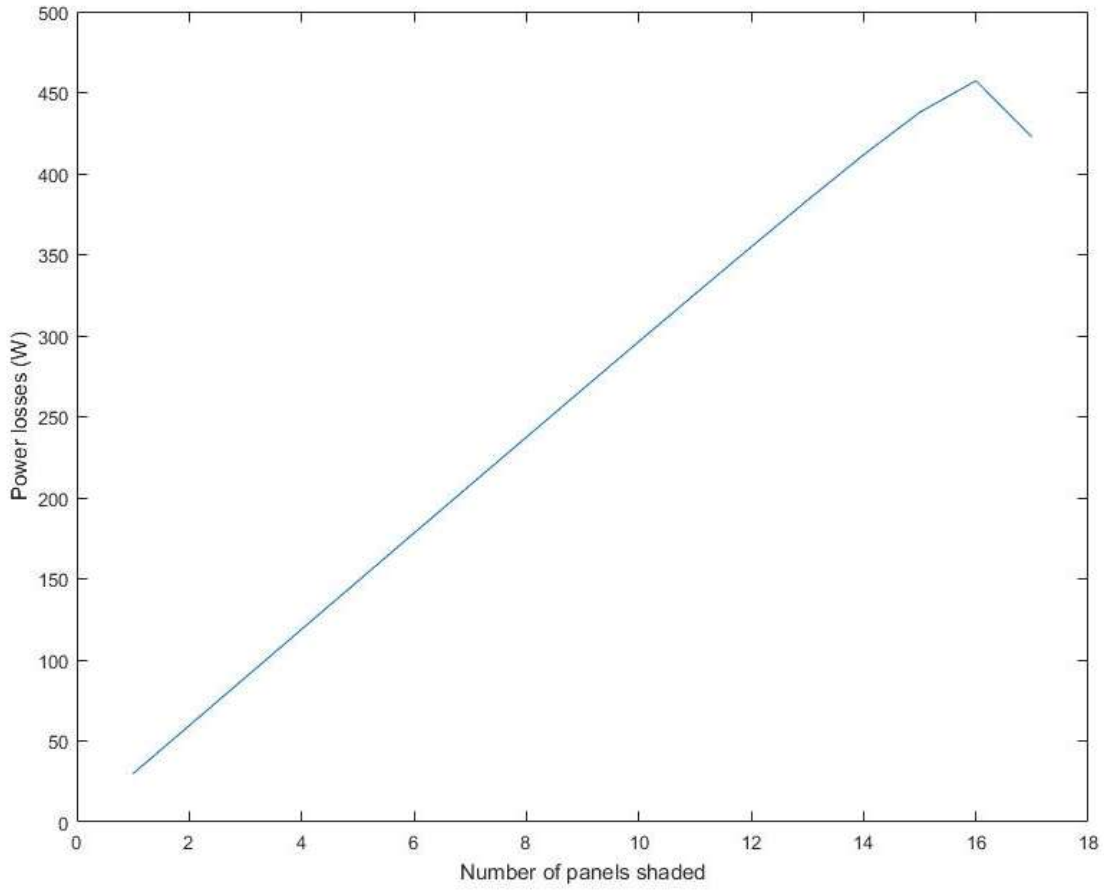

Figure 33. Mismatch power losses when the lower voltage MPP is followed. If more panels are getting shaded then the mismatch losses will get bigger.

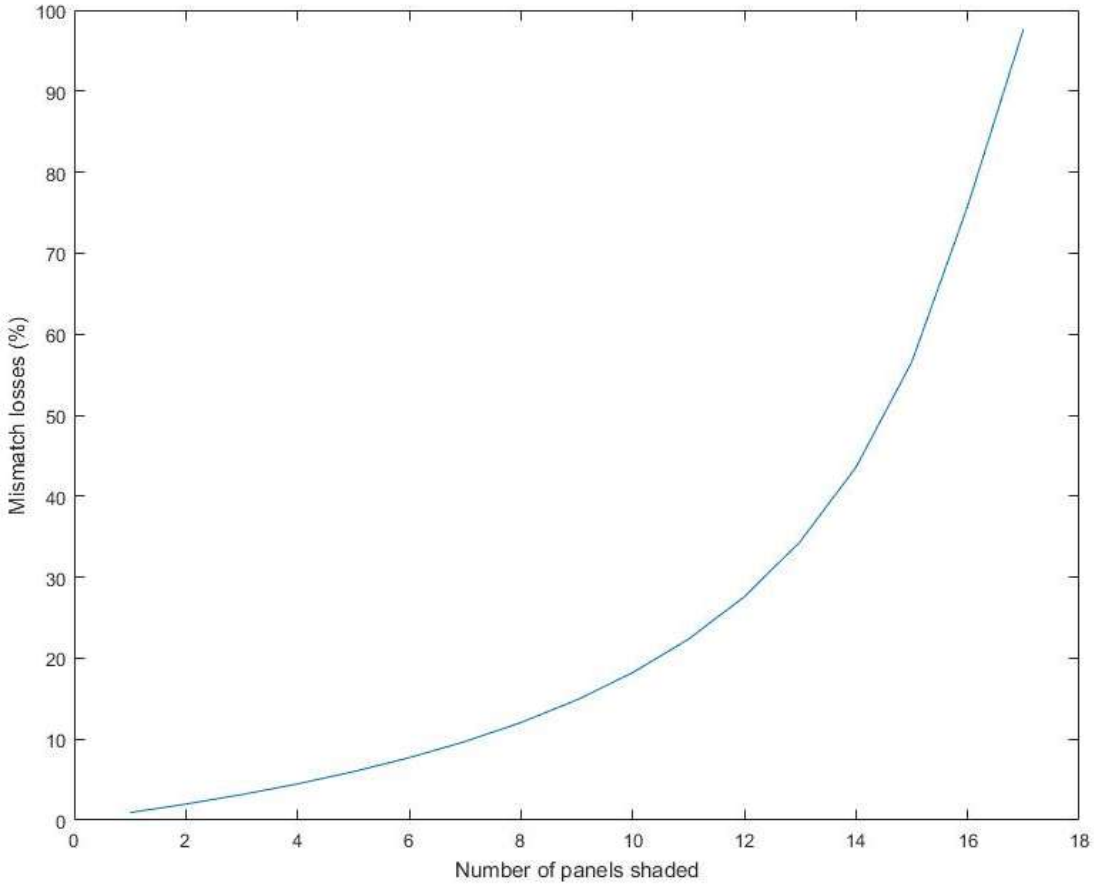

Figure 34. Relative mismatch losses when the lower voltage MPP is followed.

These results are obtained if the MPP tracking technique keeps following the low voltage MPP. But when the shadow reaches panel 16 the local MPP at high voltages becomes the global MPP. This can be seen in figure 35. If the MPP tracking follows the global MPP instead of following the first low voltage peak then the mismatch losses are different for the last 3 panels.

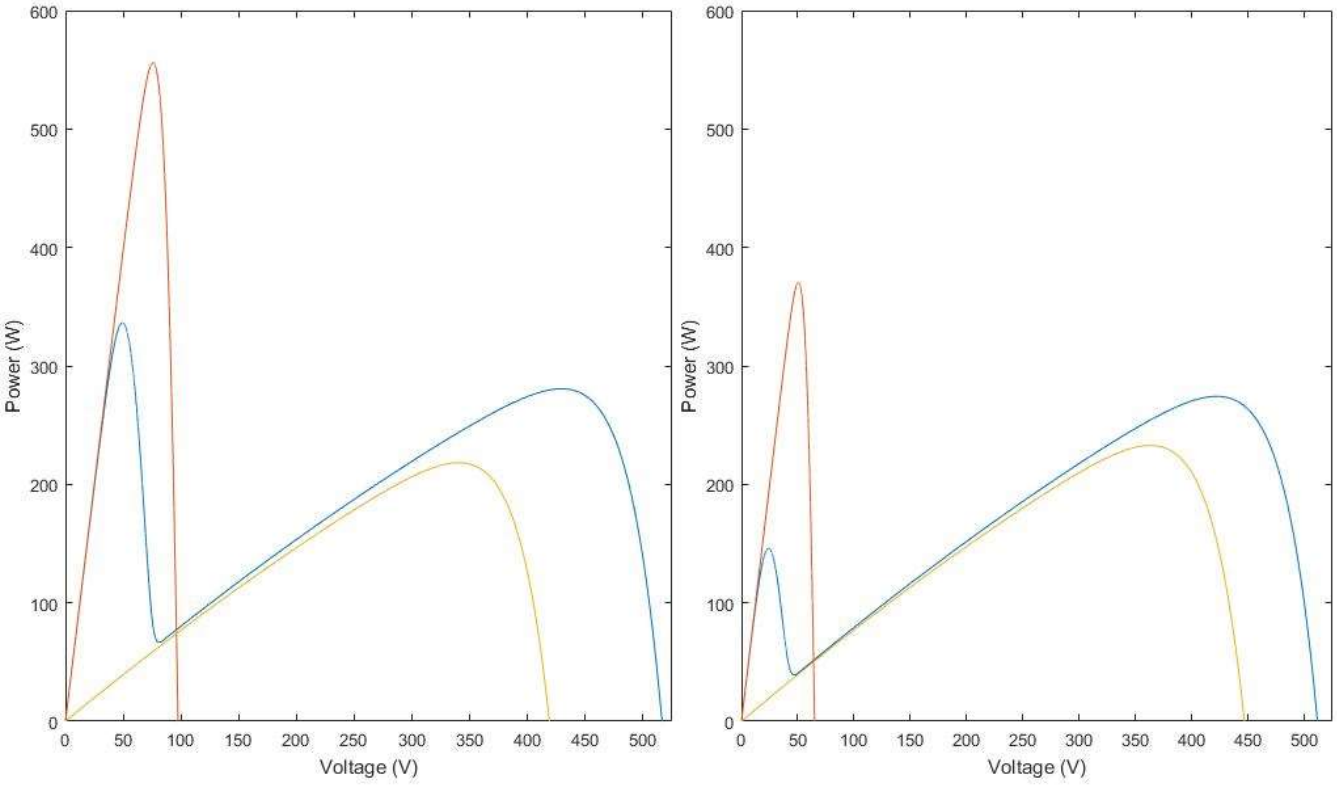

Figure 35. On the left is the voltage-power curve (blue curve) when the first 15 panels are shaded and 3 panels are unshaded and connected in series. On the right is the voltage-power curve (blue curve) when 16 panels are shaded and 2 are unshaded and connected in series. The red power curve represents the power output of the unshaded PV panels. The yellow curve is the cumulative output of the shaded cells.

The previous mismatch losses results are received when the MPPT keeps tracking the first maximum power point. If the MMPT technique is advanced enough it could track the global MPP instead. The results when the global MPP is tracked instead can be seen in figure 36 and figure 37.

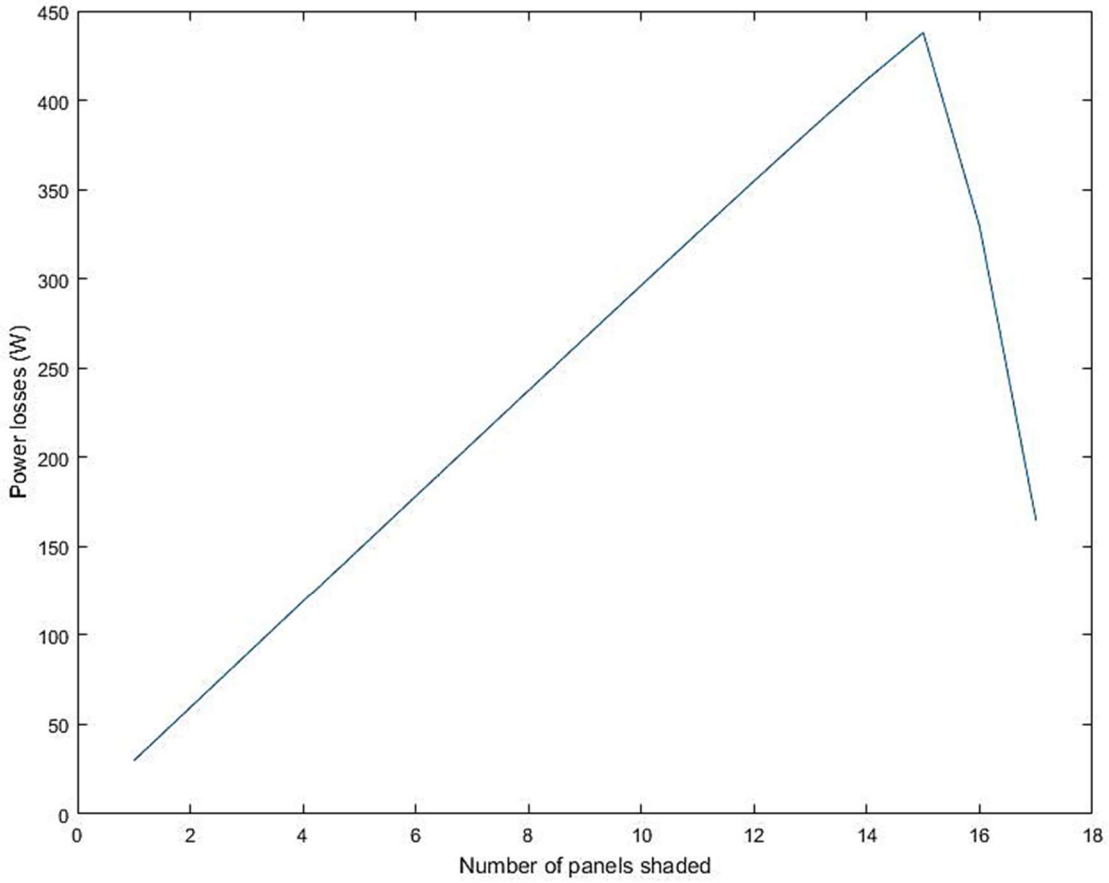

Figure 36. Mismatch losses when the global MPP is followed as a function of shaded PV panels.

These results show a descend in mismatch losses if the shadow covers more than 15 PV panels when the MPP tracking technique follows the global MPP. It is important to know that if the MPPT does not track the global MPP that these losses are not mismatch losses but partly losses due to incorrect operation of the MPP tracking algorithm. If the tracking algorithm does not follow the global MPP then the mismatch losses will be different than when it does follow the global MPP.

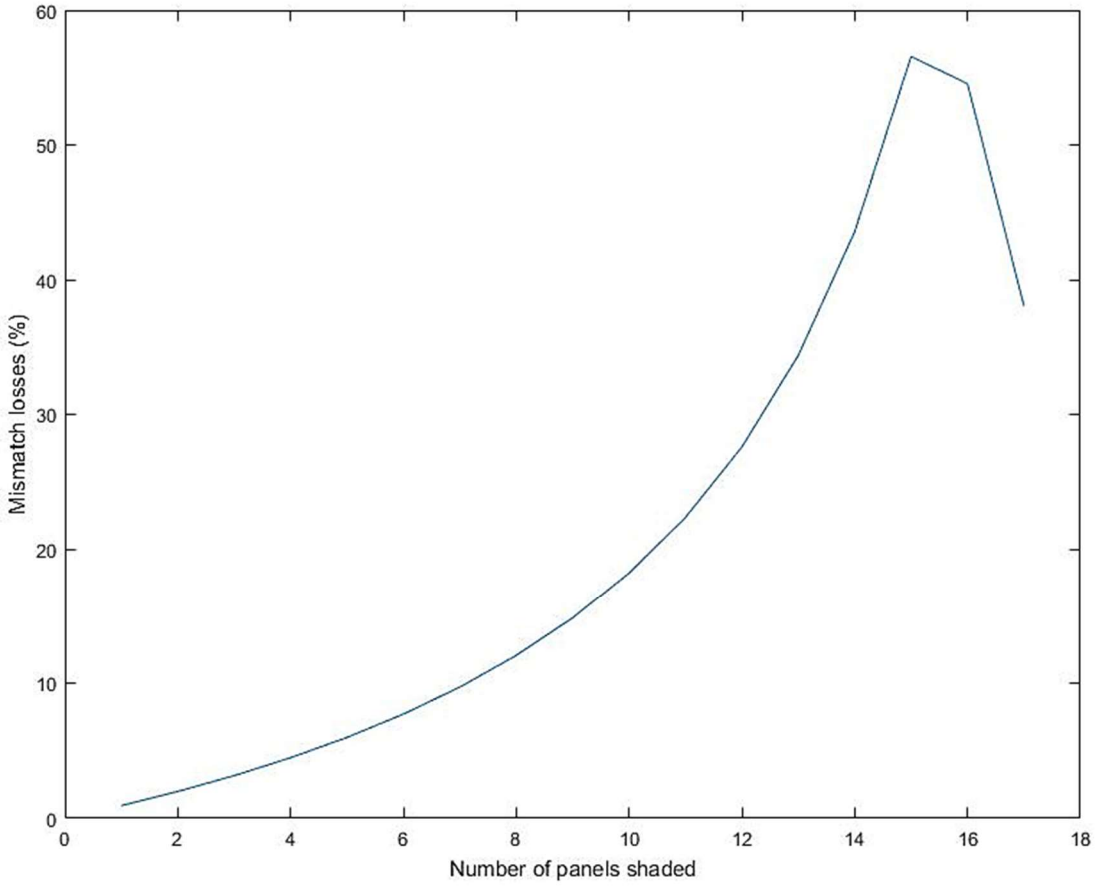

Figure 37. Relative mismatch losses as a function of shaded cells when the global MPP is followed.

4.1.4 Energy output

The goal is to compare the energy output when there is shadow caused by the building with the situation where there is no shadow. When there is no shadow the input irradiation is 1000 W/m² and fixed. The PV generator power curve as a result of the shadow is given by figure 38. This curve is a plot of the MPP power measured every 10 seconds. In figure 38 it is clearly visible how the shadow gradually starts shading the PV panels. Because the shadow is bigger than the PV installation there is also a time where the shadow keeps the PV array shaded completely.

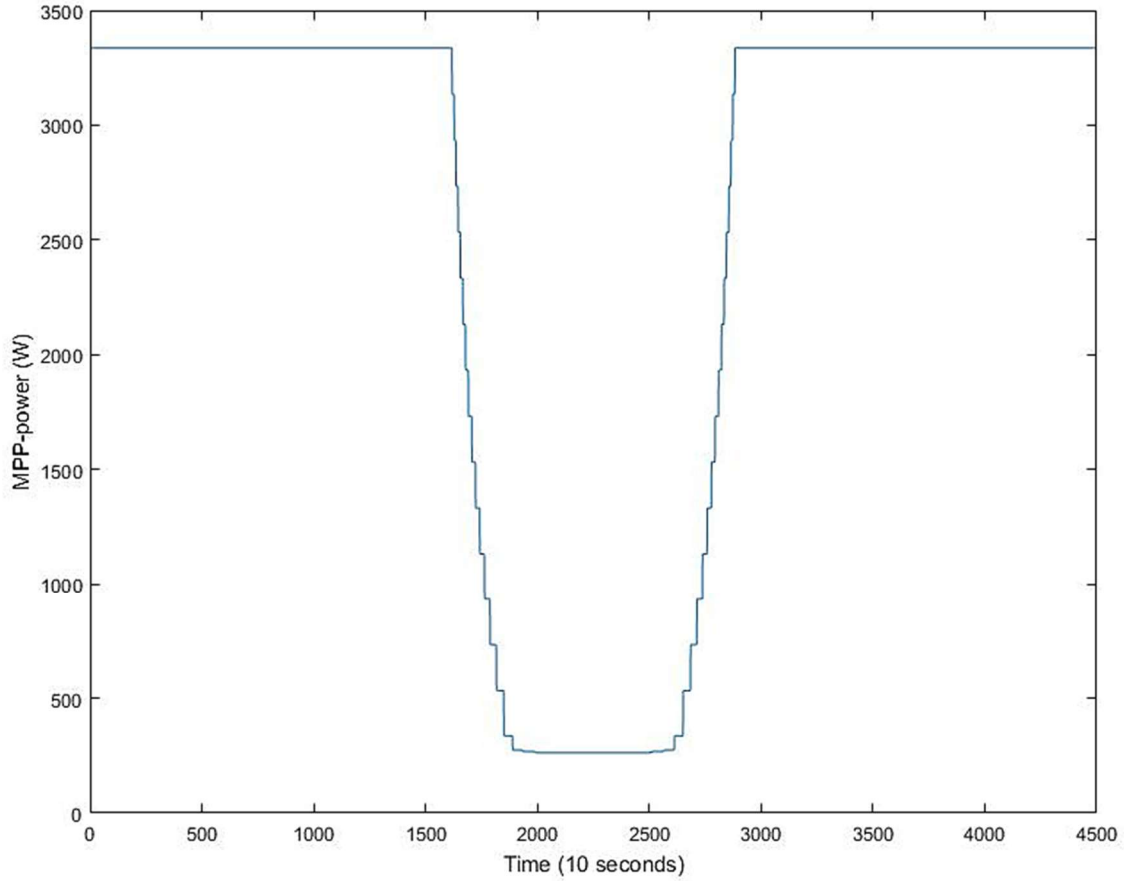

Figure 38. Simulated maximum power of the PV string generator as a function of time for 10 seconds. The implementation of the shadow is clearly visible in this figure.

If the MPPT keeps following the global MPP then the total energy received from a normal day without shadow for this 18 panel PV-string is 41.69 kWh. The total energy received from a normal day with a shadow bigger than this 18 panel PV-string is 32.38 kWh. The energy loss caused by this shadow is 22%. The energy loss is visible on figure 39.

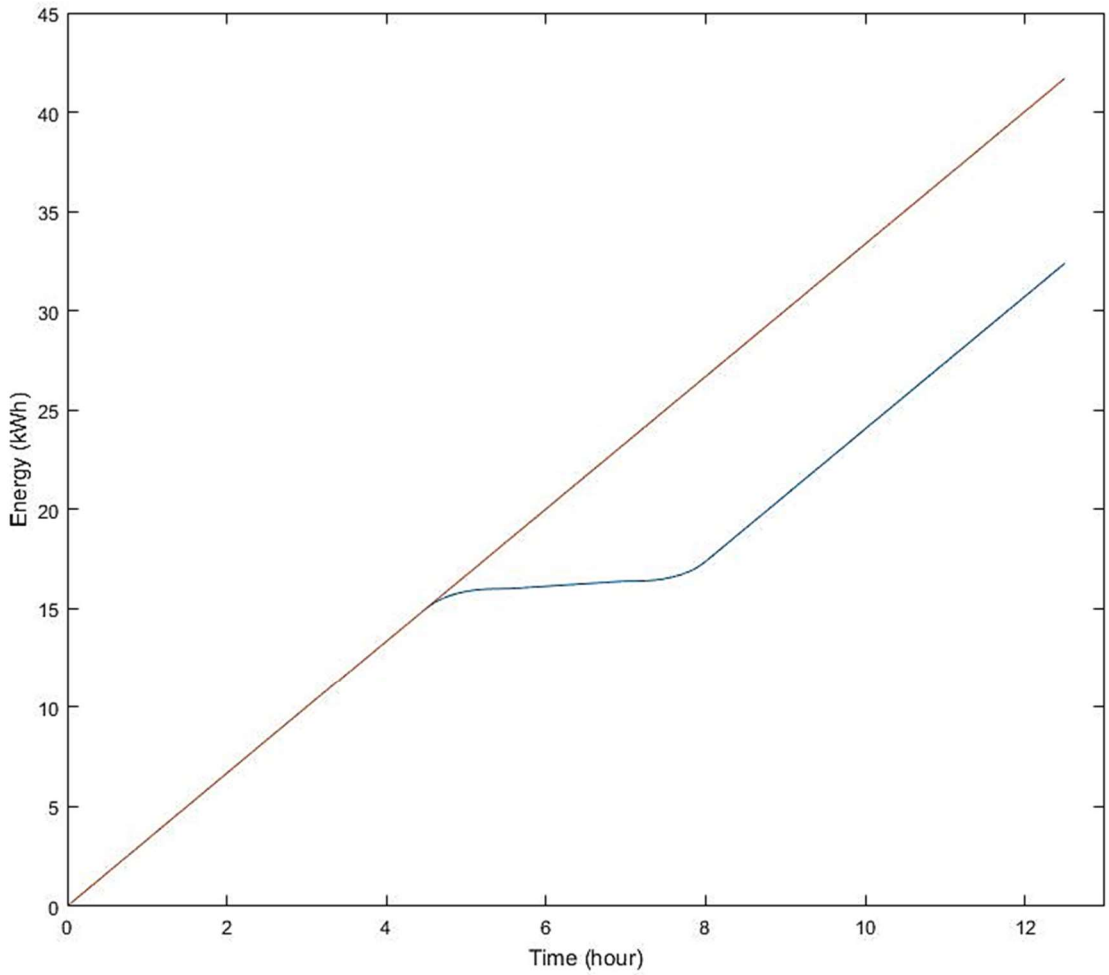

Figure 39. Energy output for the PV installation when there is a fixed irradiation of 1000 W/m² with and without shadow.

An interesting plot is the relative energy loss caused by this shadow. This is the difference in energy between the day without shadow and the day with the implemented shadow caused by the building. These relative energy losses are plotted in figure 40. The absolute value for the energy lost is 9.3 kWh.

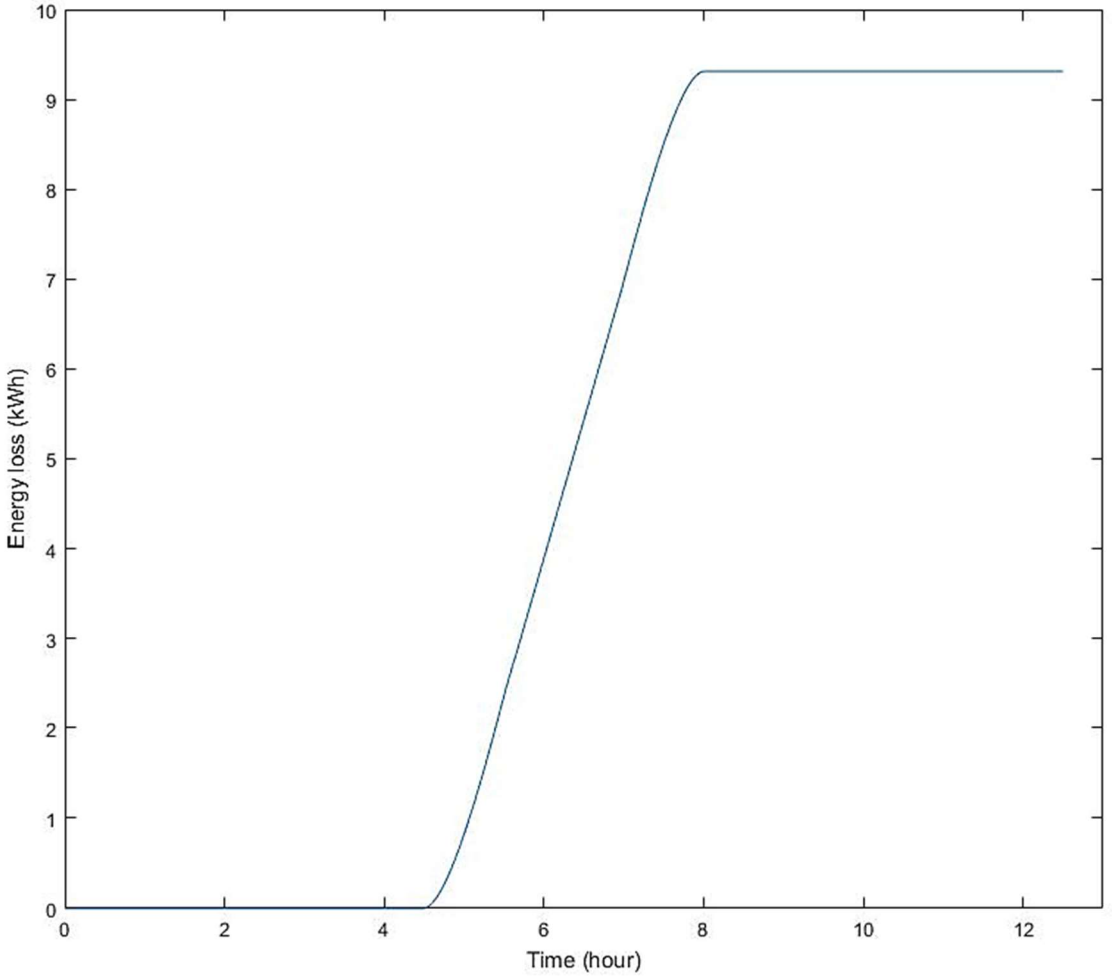

Figure 40. Relative energy loss between clear sky day without shadow caused by the building and a cloudless day with the shadow caused by the building in our system setup during the day.

4.1.5 Energy output with failing MPPT

When the shadow reaches panel 16, the once local MPP becomes the global one. These results have been handled in the paragraph “Mismatch losses” earlier in this thesis, see also figure 35. It could be interesting how much power loss is caused if the MPPT technique keeps following the first low voltage MPP instead of the global MPP of the photovoltaic installation. The total energy received when global MPP is tracked at all times is 32.49 kWh. The total energy received when first low voltage MPP is tracked at all times is 32.38 kWh. The energy loss caused by different operation of MPPT is 0.5%.

Following the first low voltage MPP instead of the global MPP does not have a big influence on the energy output of the installation. The difference in energy output is plotted in figure 41.

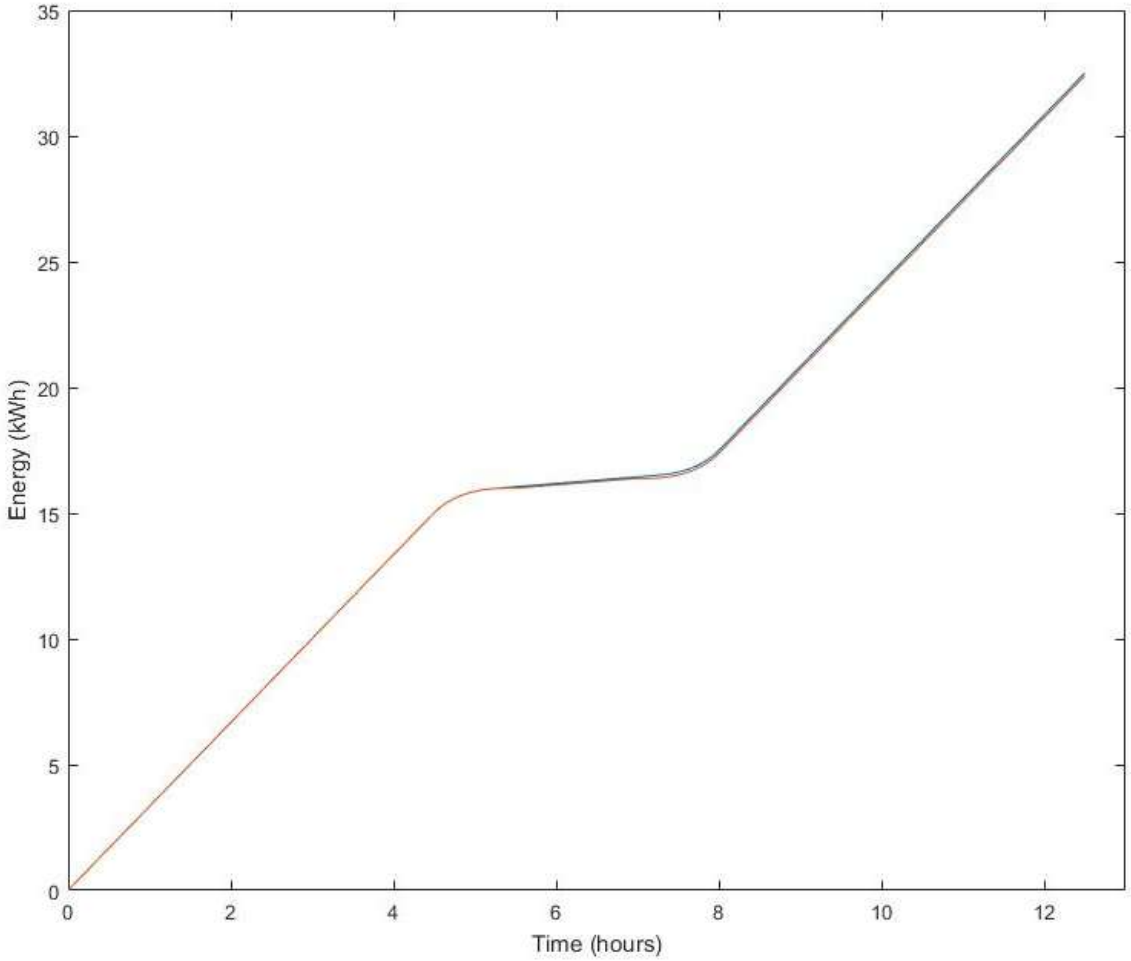

Figure 41. Difference in energy output between following the global MPP or the MPP at lower voltages.

4.2 Measured data on a clear sky day

The power output with a constant value for the irradiance of 1000 W/m² does not represent the power output when the shadow passes over the PV-array with a variable irradiance. This variable irradiance is received from measurements performed on the PV-installation on the roof of the TUT facility. It is interesting to see what influence the

shadow has on the power output when it occurs at noon. At this time the irradiance peaks and a shadow on this moment will have the most influence on the output of the PV-generator.

4.2.1 Irradiance on a clear sky day without shadow

To simulate the worst case scenario, basically when the most power losses occur, it is designated to use a beautiful day with an almost perfect irradiation curve (no clouds). An example of measured data from a day without clouds is represented in figure 42.

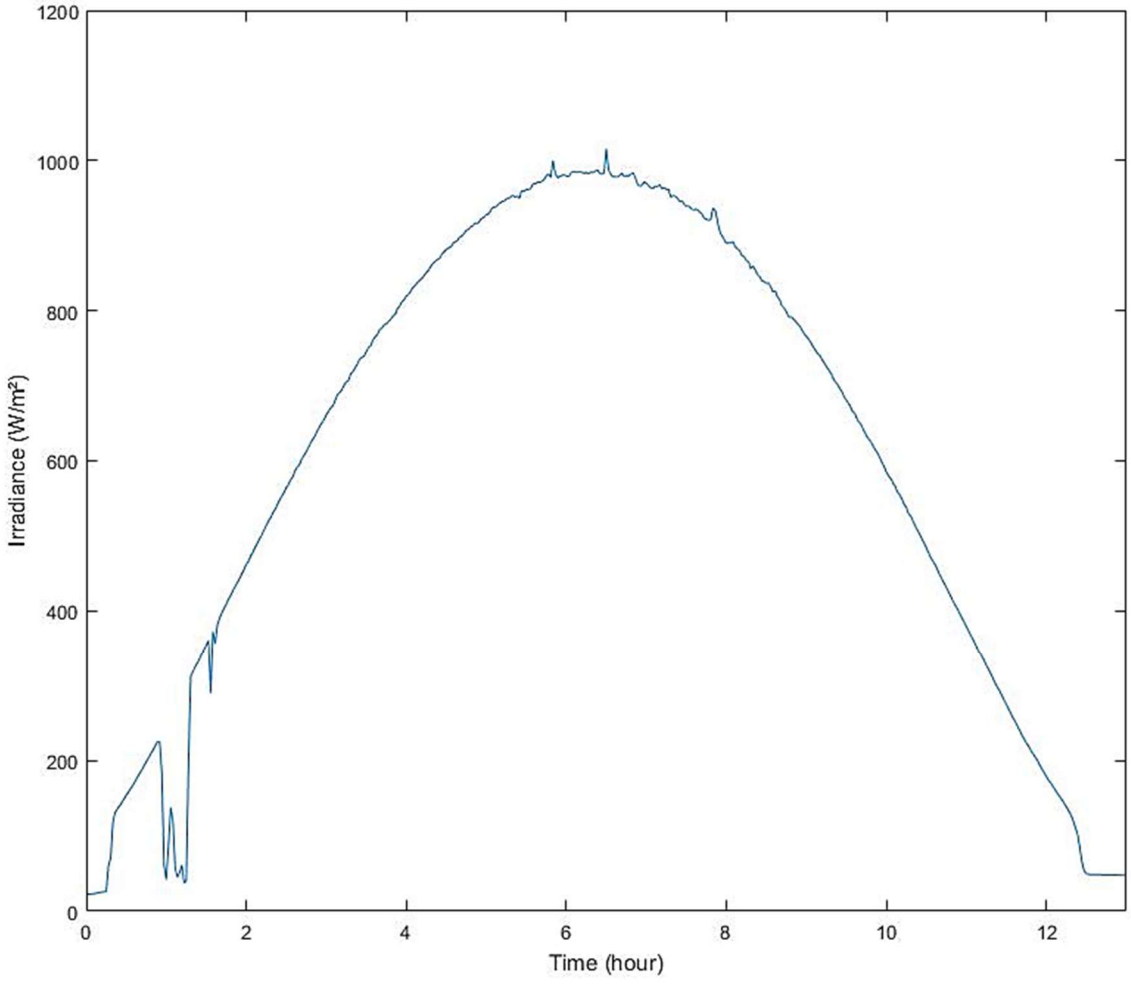

Figure 42. Example of an irradiance curve for a whole day without clouds. This data is from 21/6/2012 measured at Tampere University of Technology.

4.2.2 Implementing shadow

To implement the shadow, the amount of timesteps it takes for the shadow to fully shade the PV-array needs to be calculated. As well as how long the shadow completely shades the PV-array and how long it takes to go from completely shaded to completely unshaded. Assume that the time it takes from unshaded to fully shade the array is the same as the time it takes from shaded to fully unshade the array is the same.

It takes the shadow 4700 seconds to completely shade the PV-array. This time is the same to go back to fully unshaded as mentioned before. Since the building is bigger than the PV installation, the PV array will remain covered by shadow for a certain amount of time. At this time the whole installation only receives 10% of the irradiance and this will influence the power output a lot. The time that the PV-array stays completely covered is 3820 seconds. After implementing this time in the irradiation curve the irradiation curve as in figure 43 is received.

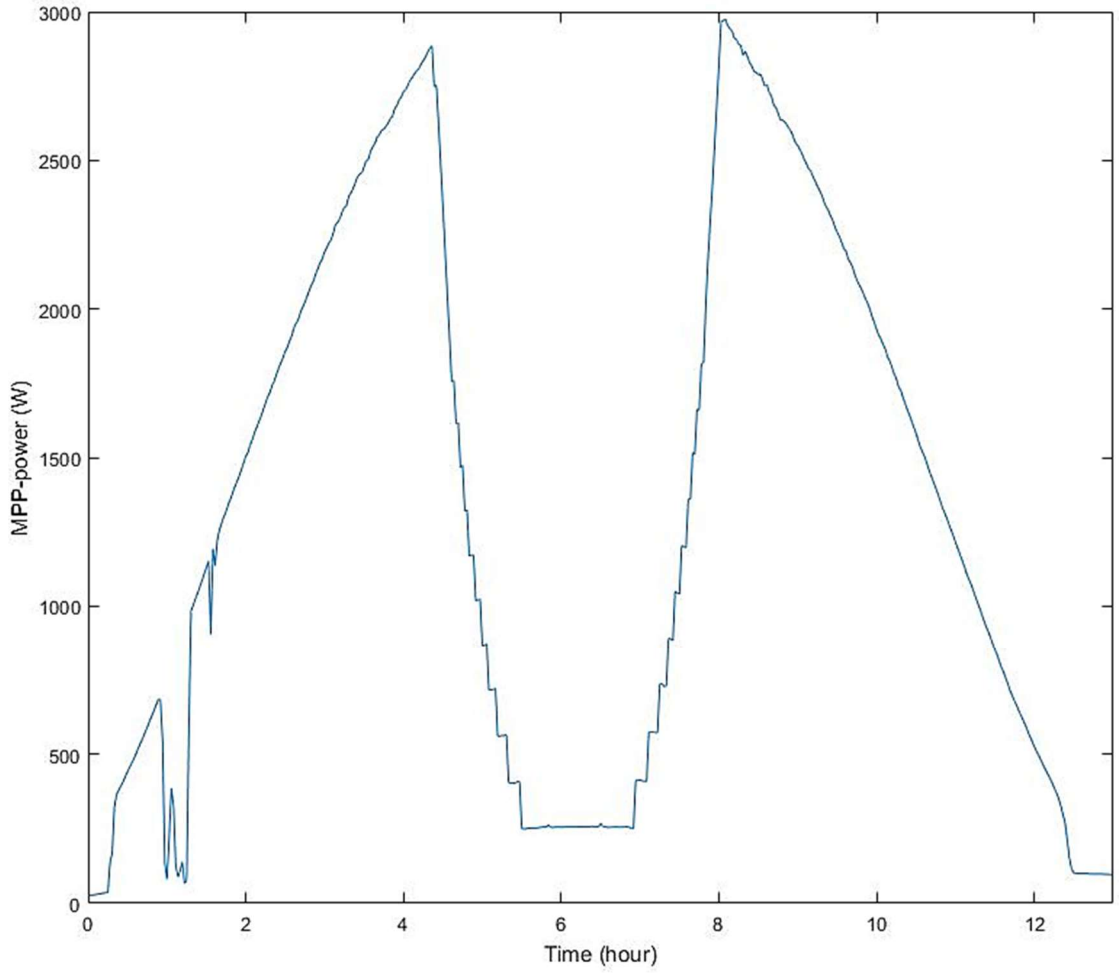

Figure 43. Maximum power curve of the PV string as a function of time when there is shadow implemented at noon. The shadow is calculated following our studied system setup in 3.2. It is visible that gradually the shadow covers the whole PV array. Around noon there is also some time where the PV installation remains completely covered in shadow.

In figure 43 it is clearly visible that the PV installation drops to lower power outputs when the shadow starts covering them. With this power curve it is simple to calculate the total energy received from the PV installation during the day.

4.2.3 Energy output

The energy received from the PV installation for a clear sky day with and without the shadow caused by the building is presented in figure 44. The total energy received from a normal day without shadow for this 18 panel PV-string is 25.92 kWh. The total energy received from a normal day with a shadow bigger than this 18 panel PV-string is 17.42 kWh. The energy loss caused by this shadow is almost 33%. Since the shadow occurs at the point with most irradiation the energy losses will be the highest.

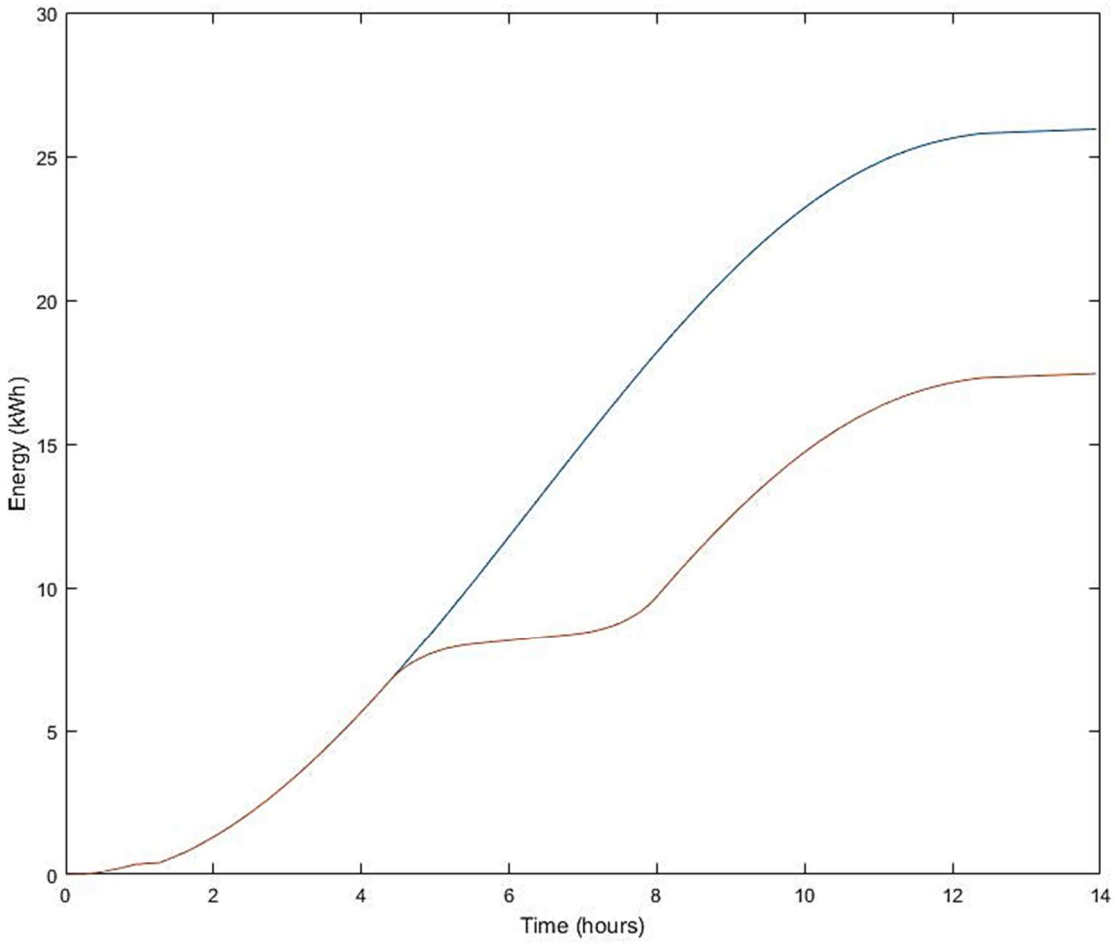

Figure 44. Total energy received from the PV installation during a clear sky day. The blue curve represents the energy output from a clear sky day without the shadow caused by the building. The red curve is the energy output when the shadow from the building is implemented on a clear sky day.

Again it is interesting to look at the relative energy losses caused by the shadow of the building (figure 45). The difference is around 8,5 kWh.

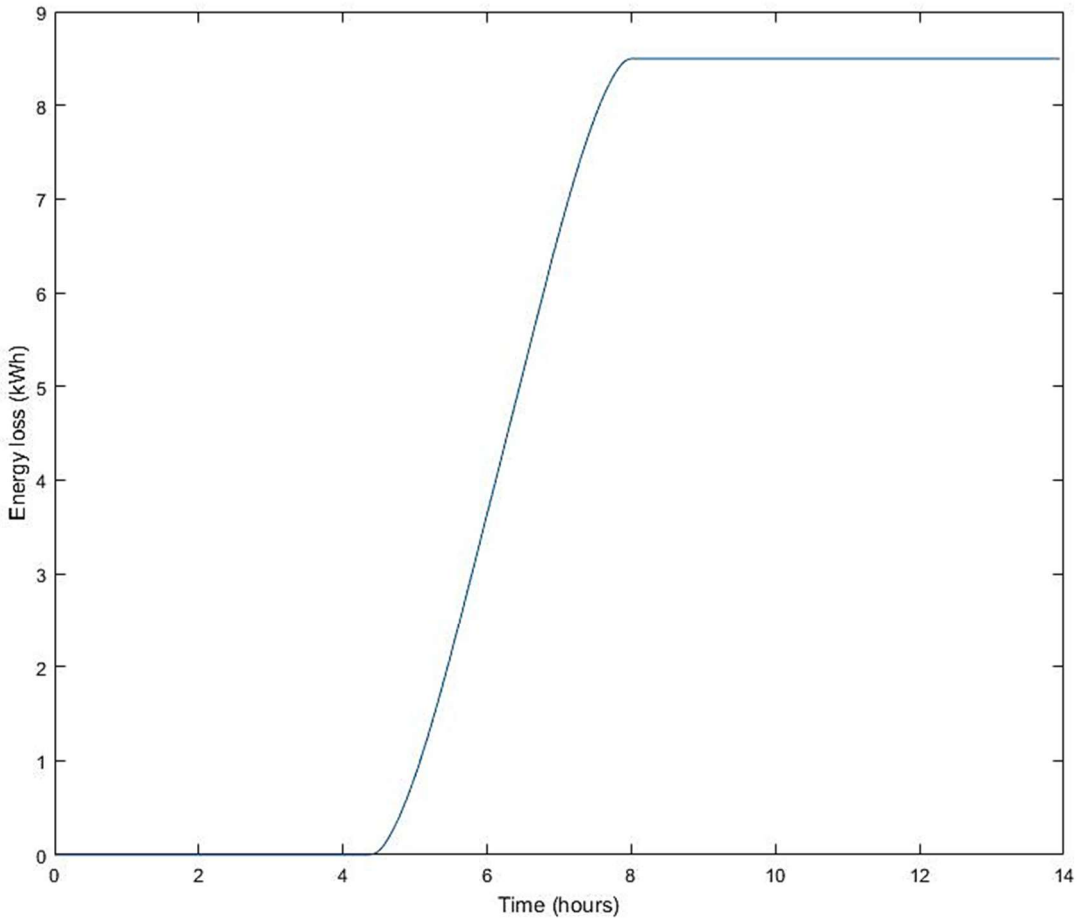

Figure 45. Relative energy loss for a clear sky day with and without the shadow caused by the building from our system setup.

4.3 Measured data on a cloudy day

A day with a lot of clouds can have an irradiation curve that looks like the graph in figure 46. If the weather would be cloudy all day then the effect of the shadow would be very small since everything is already diffuse radiation caused by the clouds. Because of this reason it is recommended to use a day with sun as well.

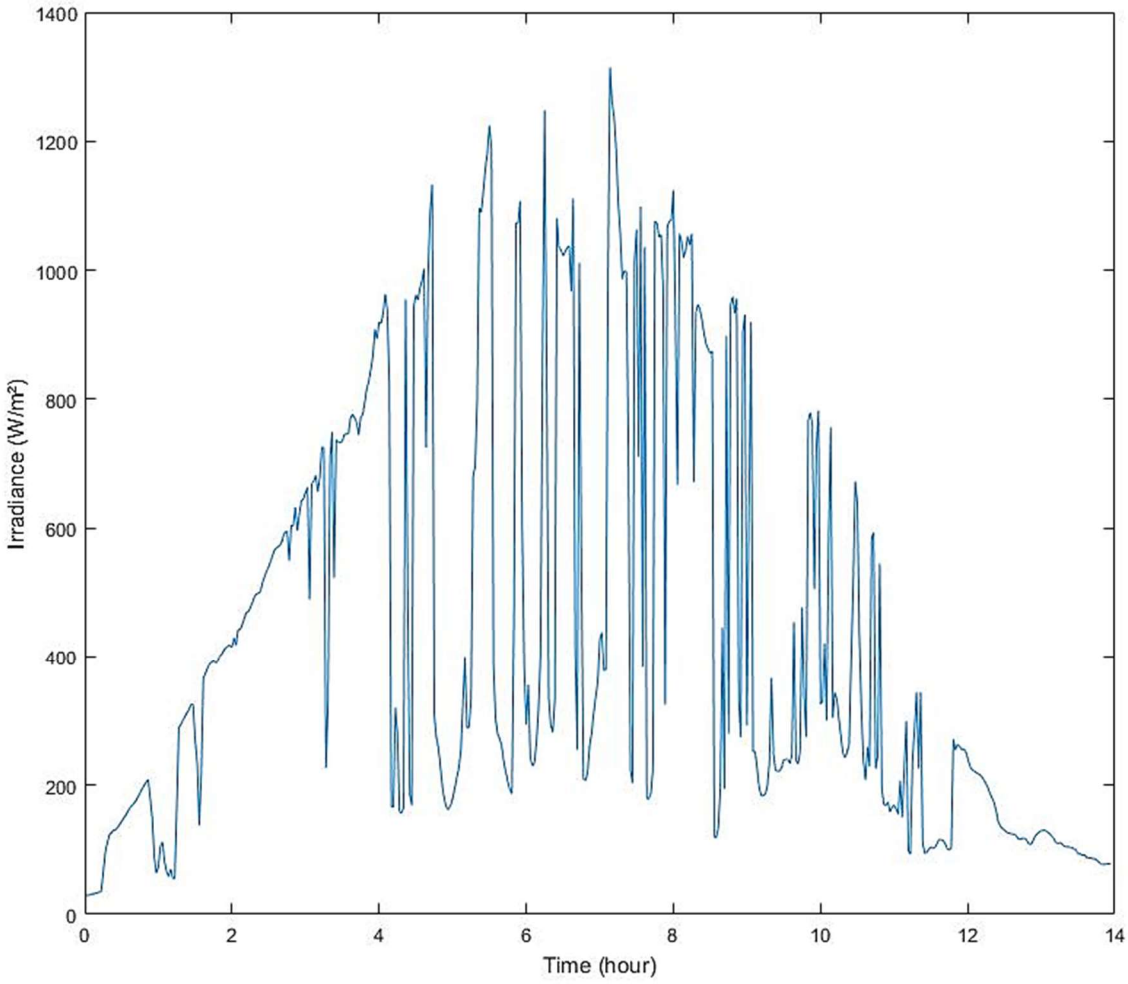

Figure 46. Irradiation curve for a half cloudy day.

4.3.1 Implementing shadow

The implementation of the shadow is parallel to the implementation of the shadow when the irradiation is a fixed value. To review the worst case of the shadow shading the PV-installation it is again recommended to simulate the shadow at noon. Because on cloudy days the amount of diffuse radiation is more than on clear sky days, where we used 10% as an estimation for the diffuse irradiation, the ratio between global irradiation and diffuse irradiation has to be estimated more precisely. To do so the data from the TUT PV installation can be consulted. The diffuse and global irradiation are given at any time so the ratio between them is known. This ratio is then used as a parameter to calculate how much irradiation is left on the PV panel when the shadow caused by the building starts shading the PV installation. In figure 52 further in this thesis the influence of a shadow on cloudy days is represented.

4.3.2 Energy output

The total energy received without shadow of a building on the cloudy day presented in figure 46 is 19.45 kWh. The total energy received when we implement the shadow of the building at noon is 17.08 kWh.

The energy loss caused by this shadow is 12% which is less compared to the clear sky day energy losses. The reason for this is that we already have losses caused by the passing clouds. On the energy output curve in figure 48 we also see that the curve is not that nicely shaped during the day as when the sky is clear in figure 44. In general the curves follow a similar path like when there are no clouds during the day.

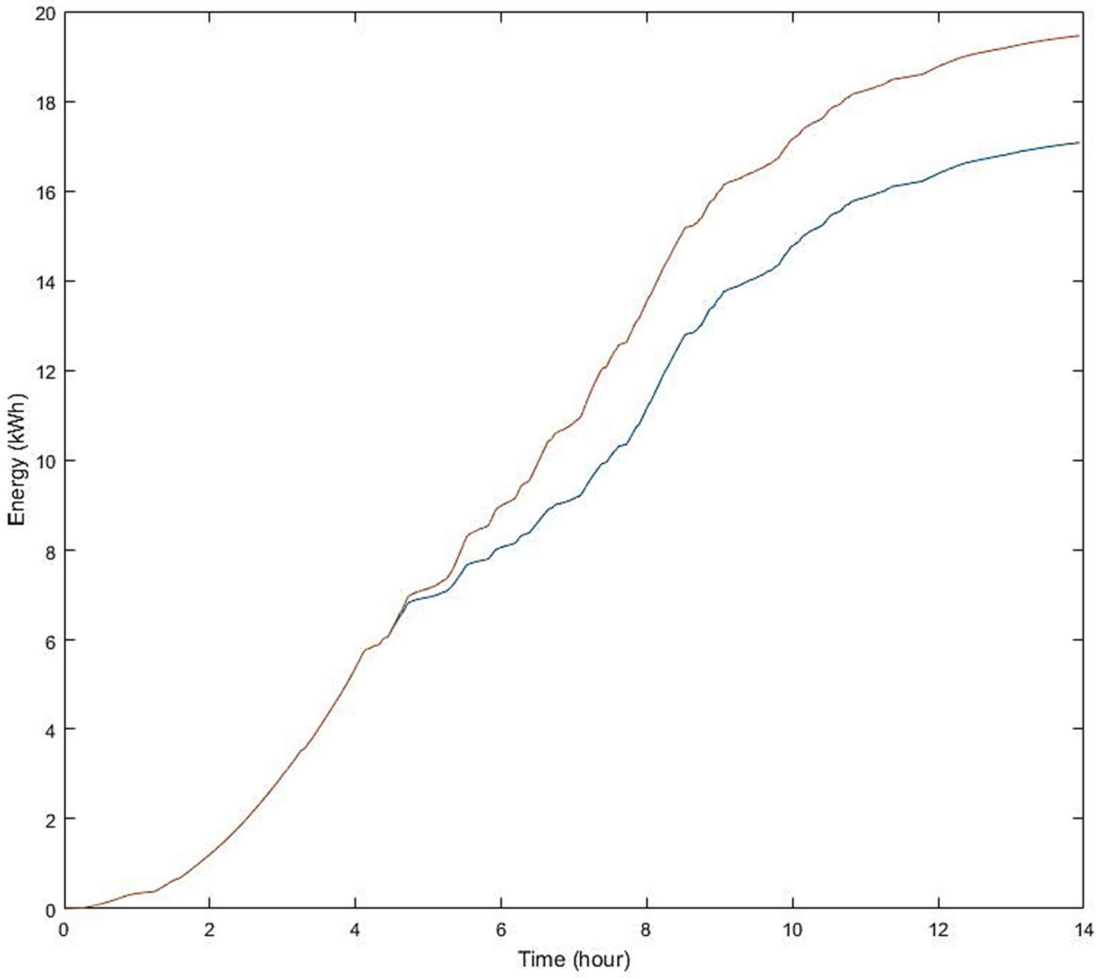

Figure 48. Total energy output on a cloudy day of figure 46. Red curve represents the energy output when there is no shadow caused by the building. The blue curve is the energy output with the shadow of the building implemented.

The absolute energy loss between a cloudy day with and without the shadow caused by the building is given by figure 49.

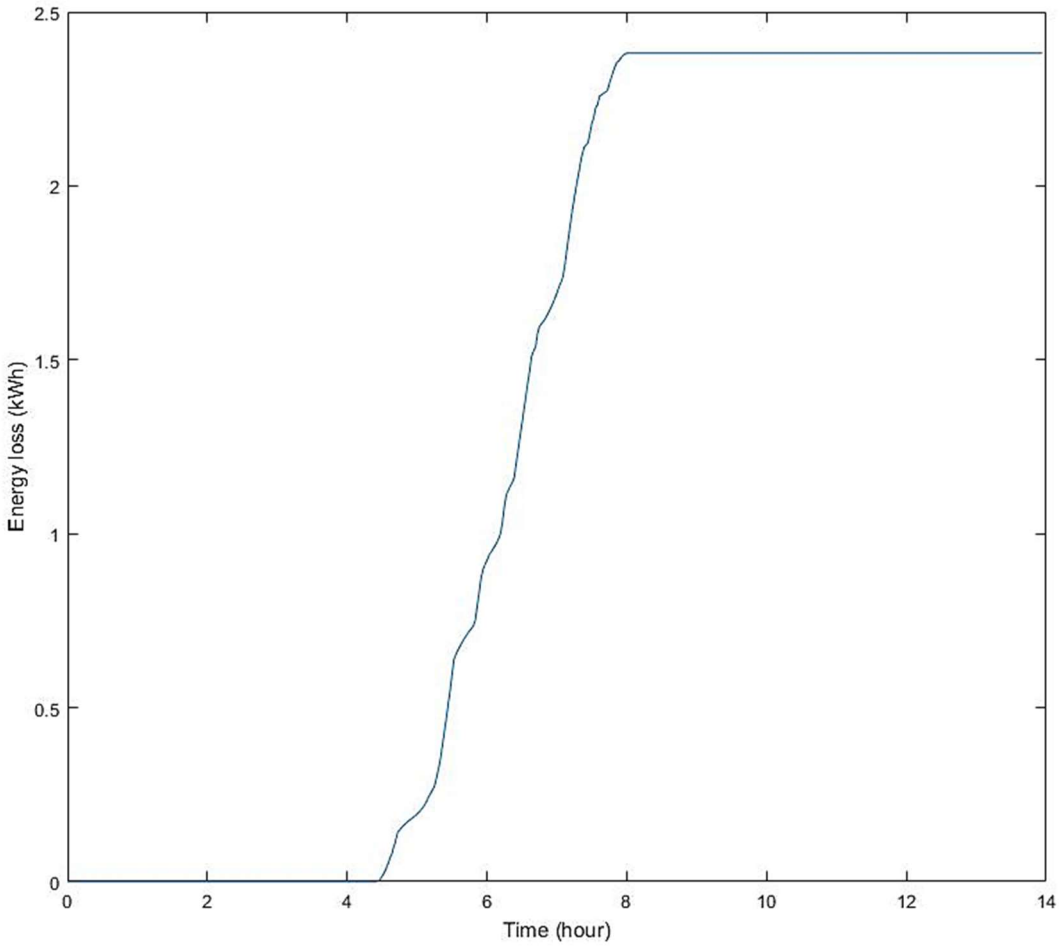

Figure 49. Absolute energy loss on a cloudy day when the shadow caused by the building is implemented in the studied system setup.

4.4 Monthly data implementation

Until now, only some specific cases were handled in this thesis. It is good to see the effects of this shadow on a sunny day and a cloudy day. This way the total energy losses caused by this particular shadow are easily readable. Although knowing these results, it would be nice to know how much energy gets lost if this shadow is present for a whole month. For this reason it is mandatory to simulate a complete month of data and implementing the shadow from our studied setup for every day during that month. In figure 50 the irradiation curve for a complete month is seen.

Because it is assumed that the angular velocity of the sun in constant, it is recommended to use a month where this angular velocity doesn't change much. The month June is perfect for this because normally June is a month with a lot of irradiation and the sunset and sunrise time doesn't change much since 21th of June is the day with the most sunlight. Instead of one day with around 500 data points, the program now works with one month and 25500 data points.

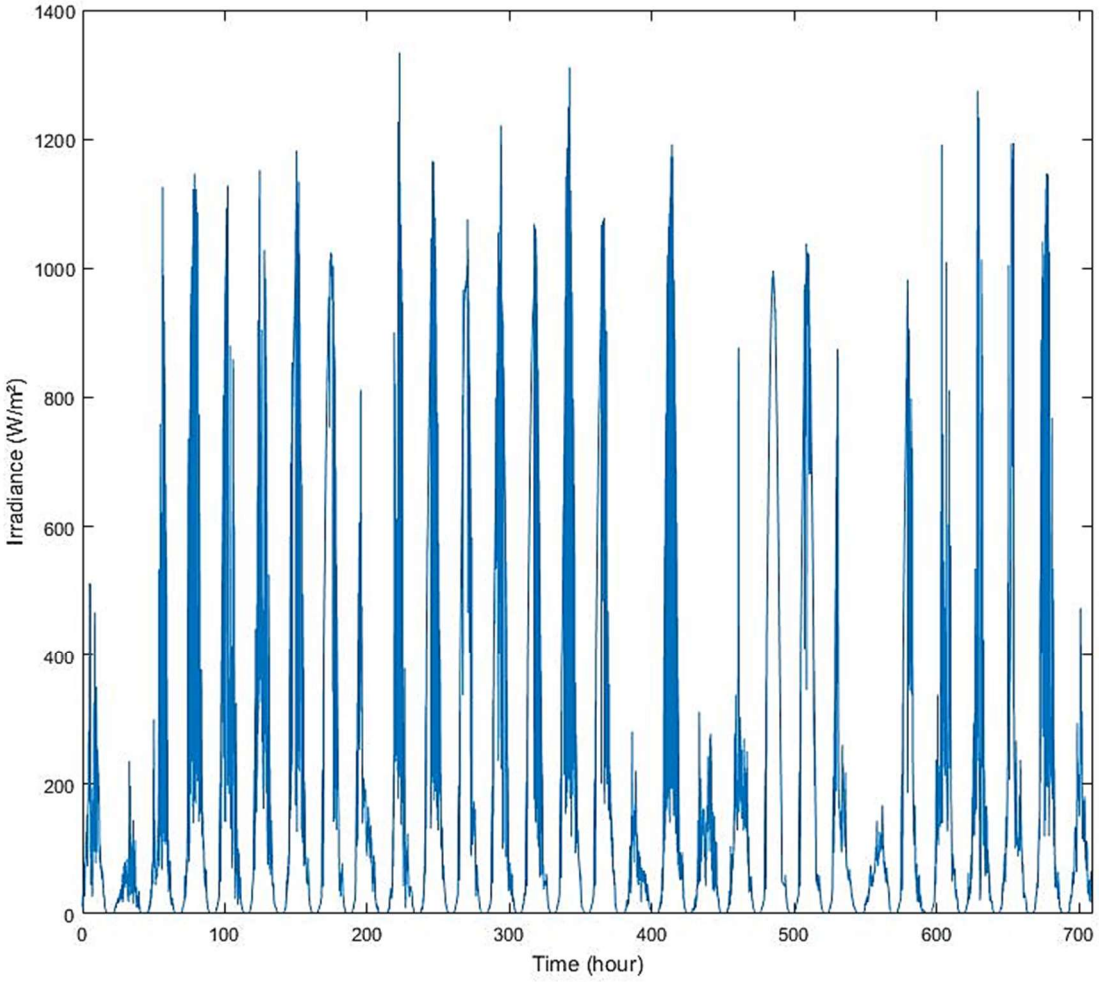

Figure 50. Irradiation curve for June 2012 measured at the Tampere University of Technology.

4.4.1 Implementing shadow

To see the difference between the original data and the implementation of the shadow we need to zoom in on some days. At first the difference for 2 almost clear sky days is examined in figure 51.

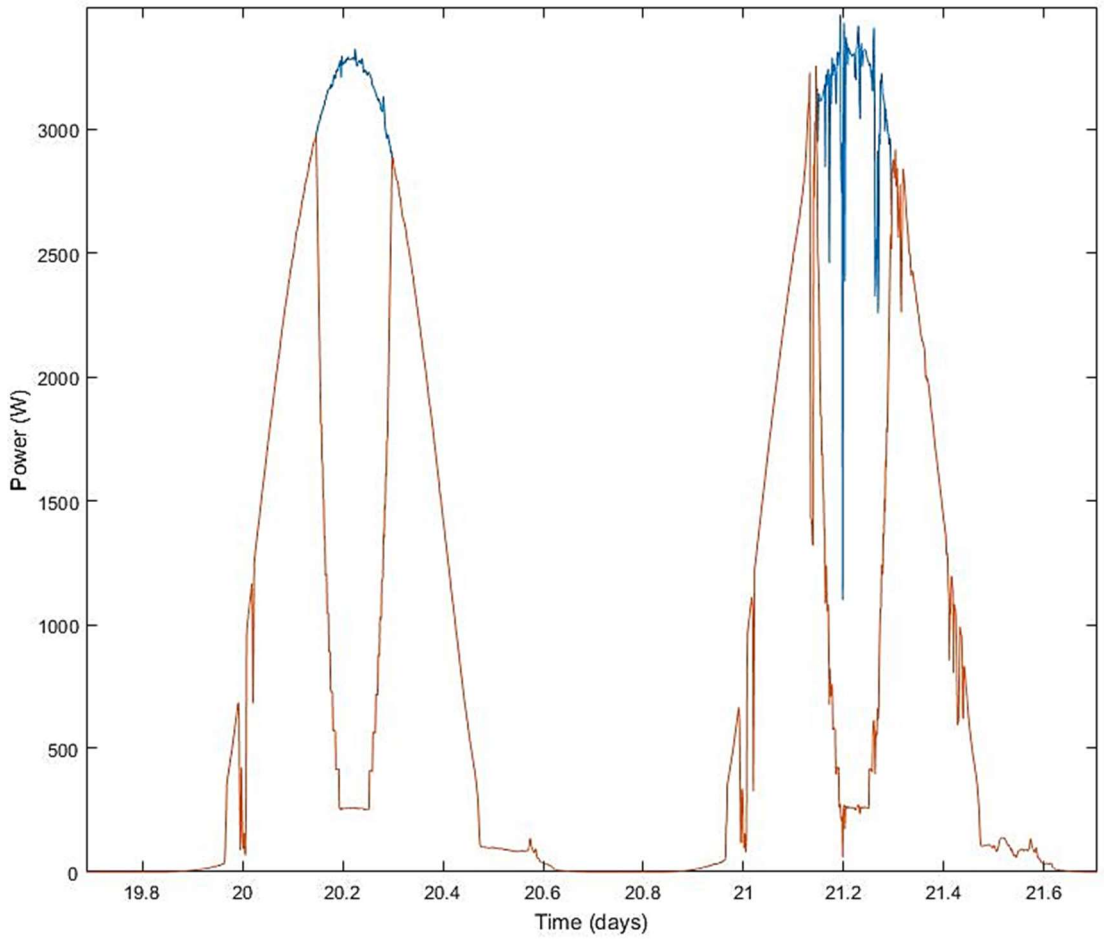

Figure 51. Power curve for 2 almost clear sky day in June 2012. The blue curve is the original data. The orange curve is the result of implementing the shadow from our studied system setup.

For cloudy days the difference between shaded and non-shaded situations is not so big. This can be seen in figure 52. The curves are close to each other because the amount of diffuse irradiation is around 85% of the global irradiation on cloudy days. This value can differ a lot, but for a cloudy day such as the 19th of June 2012 represented in figure 52, 85% is the mean of the ratios between global and diffuse irradiation. This information is gathered from the data of the TUT PV installation.

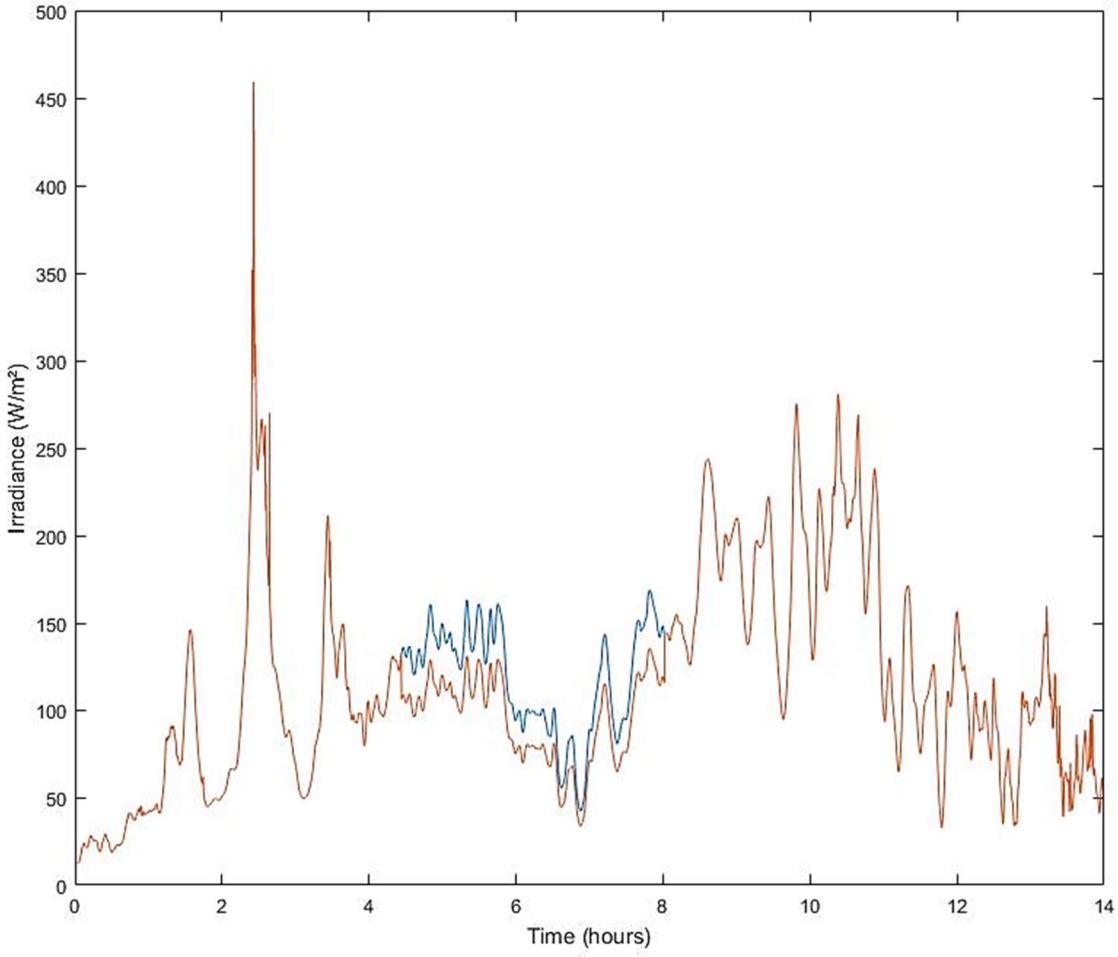

Figure 52. Difference between global irradiance (blue curve) and diffuse irradiance (red curve).

4.4.2 Energy output

The total energy received during a month when there is no shadow of a building is 433 kWh. The total energy received when we implement the shadow of the building at noon every day is 308.2 kWh. These values are visible in the total energy output curve of both conditions in figure 53.

The energy loss caused by this shadow is 28% which is a value between the losses of a clear sky day (33%) and the losses of a cloudy day (12%). This is plausible since a month of data is a collection of clear sky and cloudy days.

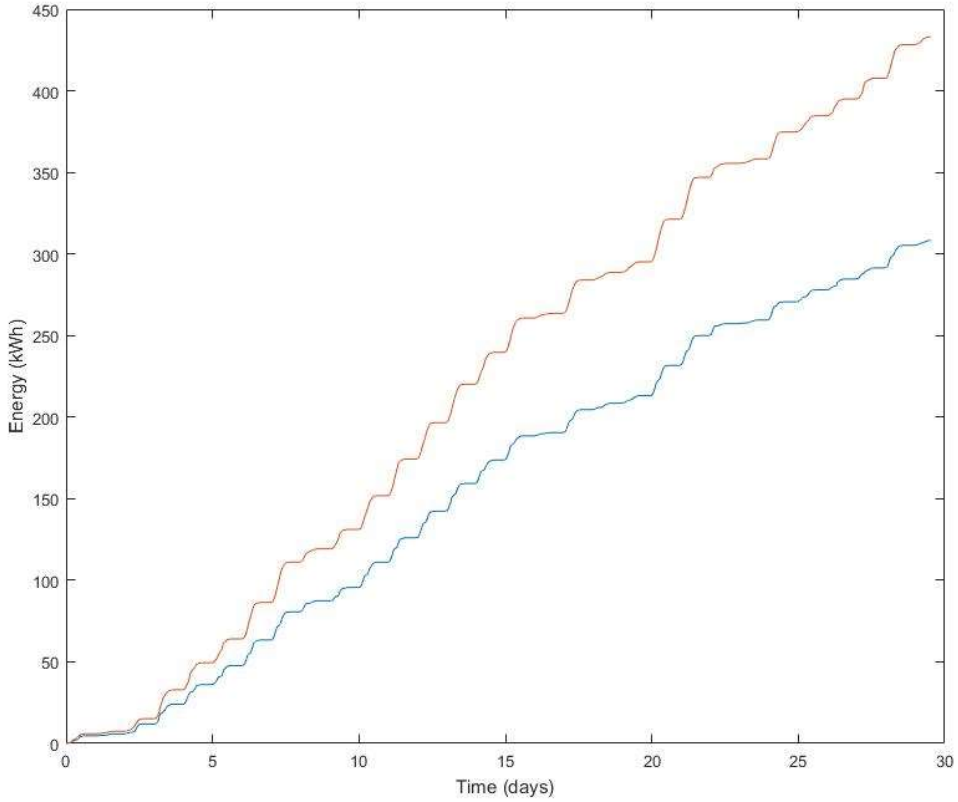

Figure 53. Total energy output for a whole month of data. The red line is the energy output without the shadow of the building. The blue line is the energy output with the implementation of the shadow.

Again it is interesting to look at the absolute energy losses in figure 54. For a whole month we have an energy loss of 124.8 kWh.

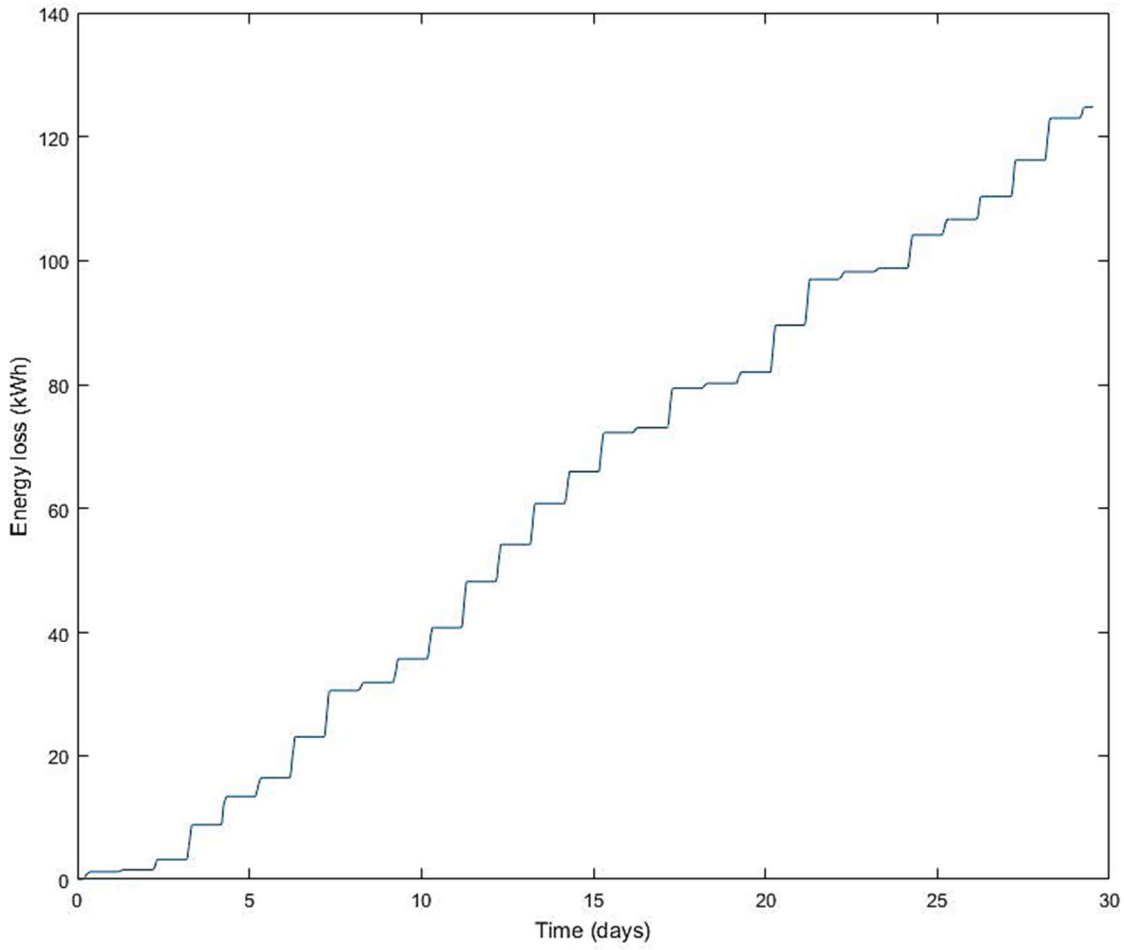

Figure 54. Absolute energy loss caused by the shadow of the building for a whole month of data.

As an overview the results from all the cases are represented in Table 4.1. The cases are fixed irradiation, clear sky day, cloudy day and a whole month. The average day for a whole month is also added and is calculated by dividing the values for the whole month by the amount of days in that month. For June 2012 this was 30.

Table 4.1 Overview of values received by the simulations.

	Energy without shadow	Energy with shadow	Energy Losses	Relative energy losses
Fixed irradiation (1000 W/m²)	41.69 kW	32.48 kW	9.313 kW	22%
Clear sky day	25.94 kW	17.44 kW	8.498 kW	33%
Cloudy day	19.44 kW	17.08 kW	2.381 kW	12%
Whole month	433 kW	308.2 kW	124.8 kW	29%
Average day for whole month	14.433 kW	10.2733 kW	4.16 kW	29%

5. CONCLUSION

The aim of this thesis was to study the effects of a shadow caused by a building on the power output of the PV generator. To do this the models from Kari Lappalainen in Simulink were used. The parametrization of these models happened according to the NAPS NP190GKg PV module. These modules are placed on the roof of Tampere University of Technology. The data used as an input for the models comes from this installation. The PV installation on the roof of the department of Electrical Engineering of TUT has stored data for the last 5 years and so different irradiance profiles were available to use as an input for the MATLAB Simulink models. For the simulations a fixed setup was used with 18 PV modules connected in series.

Three different cases were observed. First the model received a fixed irradiance input. The influence of the shadow in this case was less than the losses on a clear sky day because the irradiance in the morning and evening were kept constant at 1000 W/m². The losses caused by the shadow were 22%. When using a real irradiance profile for a clear sky day as an input for the model the losses were 33%. The same shadow was also implemented for a cloudy day. Because this day already has less power production, the losses caused by the shadow are smaller as well. For the cloudy day the losses were 12%. Because only a perfect clear sky day and a very cloudy day does not give a practical value for the losses caused by the shadow, the losses during a whole month were observed. As expected the loss percentage was somewhere between a clear sky day and a cloudy day with a value of 29%.

There are also other losses than the losses caused by the shadow. In this thesis the mismatch losses caused by the shadow gradually shading the PV installation are calculated. These losses occur when a part of the PV generator gets shaded. The more PV modules got shaded the bigger the mismatch losses (MML) were. When the global MPP was followed by the MPPT then the MML were 440 W maximum or 56%. When the MPP tracking technique follows the first MPP instead of the global MPP then the losses caused by the MPPT that fails are 0.5%. This value is very small because the MPPT failing can only happen when already 15 PV panels of the 18 are shaded and the power output at that moment is already very small.

The thesis could be more precise if there were different kinds of shadows implemented in the MATLAB program. This way the influence of the width of the shadow could also be estimated. For the results made in chapter 4 the shadow was assumed to move perpendicular to the direction of the series connection of the PV cells in the PV panel. If the program would also implement shadows that move at another angle than perpendicular to the PV cell strings, then the thesis would be even more valuable.

Other research work that also handled the topic of this thesis or is closely related to the topic of this thesis are *Partial Shadowing of Photovoltaic Arrays with Different System Configurations: Literature Review and Field Test Results* by A. Woyte, J. Nijs and R. Belmans [13] and *Determination of Energy Output Losses Due to Shading of Building-integrated Photovoltaic Arrays Using a Raytracing Technique* by A. Kovach and J. Schmid.[5]

REFERENCES

[1] Beniston, M. (2004). Natural Forcing of the Climate System. In Climatic Change and Its Impacts (pp. 53-71). Springer Netherlands.

[2] European Commission. (2016, November 23). Climate strategies & targets. Re trieved April 30, 2017, from https://ec.europa.eu/clima/policies/strategies_en

[3] Global Status Report. (2016). Retrieved May 08, 2017, from http://www.ren21.net/status-of-renewables/global-status-report/

[4] Häberlin, H. (2012). Photovoltaics system design and practice. John Wiley & Sons.

[5] Kovach, A., & Schmid, J. (1996). Determination of energy output losses due to shading of building-integrated photovoltaic arrays using a raytracing tech nique. Solar Energy, 57(2), 117-124.

[6] Lappalainen, K. (2012). Effects of climate and environmental conditions on the operation of solar photovoltaic generators.

[7] Miller, B. (n.d.). Information on Grid Connect Solar Photovoltaic systems. Re trieved April 16th, 2017, from http://www.barrymiller.com.au/solar/

[8] PhysLink.com, A. S. (n.d.). Retrieved May 02, 2017, from http://www.phys link.com/Education/AskExperts/ae24.cfm

[9] Rocheleau, J. (n.d.). Retrieved April 30, 2017, from http://planetfacts.org/what-is-the-path-of-the-sun/

[10] Smil, V. (1991). General energetics: energy in the biosphere and civilization. In General energetics: energy in the biosphere and civilization. John Wiley & Sons.

[11] Tampere, Finland - Sunrise, Sunset, and Daylength, June 2012. (n.d.). Retrieved March 12th, 2017, from https://www.timeanddate.com/sun/finland/tam pere?month=6&year=2012

[12] Valkealahti, S. Course Study Material: DEE-53117 Solar Power Systems. Tam pere University of Technology. Retrieved on February 10th 2017 from http://webhotel2.tut.fi/units/set/opetus/kurssit/DEE_53117/index.html

[13] Woyte, A., Nijs, J., & Belmans, R. (2003). Partial shadowing of photovoltaic ar rays with different system configurations: literature review and field test re sults. Solar energy, 74(3), 217-233.

The referencing style used for in-text citations is according to the Harvard system. The reference style used in “References” is in APA style. (n.d. means non determined)